LONG-TERM POTENTIOSTATIC EXPOSURES OF 304 STAINLESS STEEL AT ELEVATED TEMPERATURES

By

JANE-FRANCES NANNYOMO BAKAMA

Bachelor of Science

Oklahoma State University

Stillwater, Oklahoma

1983

Submitted to the Faculty of the Graduate College
of the Oklahoma State University
in partial fulfillment of the requirements
for the Degree of
MASTER OF SCIENCE
July, 1985

LONG-TERM POTENTIOSTATIC EXPOSURES

OF 304 STAINLESS STEEL AT

ELEVATED TEMPERATURES

Thesis Approved:

Robert H Heidersbach Jr

Thesis Adviser

Mayis Seapan

Archibald A Hill

Norman N. Durham

Dean of the Graduate College

PREFACE

Stainless steels suffer from pitting and crevice corrosion in chloride environments. This localized corrosion can be prevented by determining a protection potential below which metals will not corrode by pitting or crevice corrosion. Above this potential, crevice corrosion will occur, but pitting will not initiate until the rupture potential is reached.

The purpose of this experiment was to determine the protection potential of 304 stainless steel at elevated temperatures using two electrochemical techniques. The electrochemical hysteresis technique, which involves a reverse potentiodynamic scan in the active direction, was first used to identify the protection potential. The protection potential was then verified by long-term immersion of samples in different environments at fixed potentials 50 mV below or above the potentiodynamically-determined value.

I wish to express my sincere gratitude to Dr. Robert H. Heidersbach, my major adviser, for his friendship, guidance, assistance and encouragement throughout my studies and preparation of this thesis.

I am also thankful to the other commitee members, Dr. Mayis Seapan and Dr. Arch G. Hill, for their advice and assistance.

Thanks are extended to the entire faculty and staff of the School of Chemical Engineering, particularly Mr. Charles Baker for his support, friendship and help throughout my years at Oklahoma State University.

Grateful recognition is extended to Rhonda Tate for typing this manuscript.

Gratitude is expressed to the School of Chemical Engineering, Holy Trinity Episcopal Church (Wyoming, Michigan), and African Enterprise for their financial assistance.

Sincere thanks for constant encouragement in the pursuit of this degree goes to two special friends, John Mburu Marenga and Tim Stieg.

Acknowledgements would not be complete without the expression of my appreciation to my host family, Mr. and Mrs. Wylie, my mother, Gertulide Nannyonga, my aunt, Dr. Jane-Frances Kamya, my grandmother, Tecla Namayanja and all other members of the family for their love and encouragement. To my loving father, Mathias Bakama, for his understanding and encouragement, I give my most sincere thanks and gratitude.

TABLE OF CONTENTS

LIST OF TABLES

LIST OF FIGURES

LIST OF FIGURES (continued)

LIST OF SYMBOLS

E_p	- Protection potential
E_{corr}	- Corrosion potential
E_{pp}	- Primary passivation potential
i_{corr}	- Current density at E_{corr}
E_r	- Rupture potential or pitting potential
E_A	- Potential 50 mV above E_p
E_B	- Potential 50 mV below E_p
SCE	- Standard Calomel Electrode
SHE	- Standard Hydrogen Electrode
NA/CM^2	- Nanoamperes

CHAPTER I

INTRODUCTION

The amount of money spent in an industrial country in combating corrosion by preventative measures is extremely high. Estimates of this sum, just for United States alone, come to $140 billion dollars per annum which is approximately 4% of the National Gross Product (1). The cost is enormous because corrosion occurs with varying degrees of severity, in practically all cases where metals and alloys are used. Aside from the cost in dollars, corrosion is a serious problem because it directly contributes to the depletion of natural resources.

Stainless Steels

The main reason for the use of the stainless steels is their resistance to corrosion. Stainless steels derive their corrosion resistance from the fact that they are passive. A metal is said to be passive in a certain environment if it shows a very low corrosion rate, when thermodynamically it would be expected to corrode rapidly (2). The corrosion resistance of all stainless steels rests upon the high chromium content. Chromium is the main alloying element, and stainless steels should contain at least 11% chromium (2). The higher the chromium content, the more resistant the steel is to oxidizing media and high temperature oxidation. Many other elements are added to stainless steels to provide specific properties or ease of fabrication. For example,

nickel and molybdenum are added for corrosion resistance, carbon and copper for strength, sulfur and selenium for machinability, and nickel for formability and toughness (3). Molybdenum is also beneficial for reducing chloride pitting.

There are four groups of stainless alloys: austenitic (face centered cubic), ferritic (body centered cubic), martensitic (body centered tetragonal), and precipitation-hardening stainless steels. Table I lists the compositions of most of the common stainless steels and the four groups of these materials.

Group I materials are termed martensitic stainless steels because they can be hardened by heat treatment and form martensite (2). Martensitic alloys contain 12 to 20 percent chromium with controlled amounts of carbon and other additives. Corrosion resistance is inferior to that of austenitic stainless steels, and martensitic steels are generally used in mildly corrosive environments.

Group II ferritic stainless steels contain between 11 and 27 percent chromium, with low carbon content. This class is so named because the crystal structure of the steel is the same as that of iron at room temperature. The higher chromium content improves corrosion resistance. The strength of ferritic stainless steels can be increased by cold working but not by heat treatment. Corrosion resistance, especially resistance to stress corrosion, is good. Ferritic stainless steels do quite well in many cases where the 18-8 austenitic types fail, particularly in chloride containing waters.

The most corrosion resistant of the four stainless steel groups are the Group III austenitic steels. These steels contain 16 to 26 percent chromium and 3 to 22 percent nickel (2). Nickel greatly improves the

TABLE I

CHEMICAL COMPOSITIONS OF
STAINLESS STEELS (2)

AISI type	%C	%Cr	%Ni	% other elements
		GROUP I		
		Martensitic Chromium Steels		
410	0.15 max	11.5-13.5	-	-
416	0.15 max	12-14	-	-
420	0.35-0.45	12-14	-	-
431	0.2 max	15-17	1.25-2.5	-
440A	0.60-0.75	16-18	-	-
		GROUP II		
		Ferritic Nonhardenable Steels		
405	0.8 max	11.5-14.5	0.5 max	0.1-0.3 Al
430	0.12 max	14-18	0.5 max	-
442	0.25 max	18-23	0.5 max	-
446	0.20 max	23-27	0.5 max	0.25 N max

TABLE I (Continued)

AISI type	%C	%Cr	%NI	%other elements
		GROUP III		
		Austenitic Chromium - Nickel Steels		
201	0.15 max	16-18	3.5-5.5	5.0-7.5 Mn
202	0.15 max	17-19	4-6	7.5-10 Mn
301	0.15 max	16-18	6-8	2 Mn max
302	0.15 max	17-19	8-10	2 Mn max
302B	0.15 max	17-19	8-10	2-3 Si
304	0.08 max	18-20	8-12	1 Si max
304L	0.03 max	18-20	8-12	1 Si max
308	0.08 max	19-21	10-12	1 Si max
309	0.2 max	22-24	12-15	1 Si max
309S	0.08 max	22-24	12-15	1 Si max
310	0.25 max	24-26	19-22	1.5 Si max
310S	0.08 max	24-26	19-22	1.5 Si max
314	0.25 max	23-26	19-22	1.5-3.0
316	0.10 max	16-18	10-14	2-3 Mo
316L	0.03 max	16-18	10-14	2-3 Mo
317	0.08 max	18-20	11-14	3-4 Mo
321	0.08 max	17-19	8-11	Ti 4 x C (min)
347	0.08 max	17-19	9-13	Cb + Ta 10 x C (min)
Alloy 20*	0.07 max	29	20	3.25 Cu, 2.25 Mo

Table I (Continued)

AISI type	%C	%Cr	%Ni	%other elements
		GROUP IV		
		Age - Hardenable Steels		
322	0.07	17	7	0.07 Ti, 0.2 Al
17-7 PH+	0.07	17	7	1.0 Al
17-4 PH+	0.05	16.5	4.25	4.0 Cu
14.8 Mo PH+	0.05 max	14	8.5	2.5 Mo, 1% Al
Am 350	0.10	16.5	4.3	2.75 Mo
CD4M Cu++	0.03	25	5	3.0 Cu, 2.0 Mo

* Typical compositions

\+ Commercial designations

++ Cast form only

corrosion resistance of stainless steels. Carbon is kept low to minimize carbide precipitation. These alloys can be work-hardened, but heat treatment cannot cause hardening. Austenitic steels are tough and ductile.

When it comes to corrosion resistance in relatively severe environments, it is generally accepted that the austenitic stainless steels are superior. The most widely used austenitic stainless steel is the type generally referred to as 18-8, meaning an iron alloy containing approximately 18% Cr and 8% Ni. 18-8 has been further divided into two types that contain, respectively, a maximum of 0.08% C (type 304), and a maximum of 0.15% C (type 302). The lower the carbon content, the less will be the danger of loss of corrosion resistance associated with heating during fabrication and use. The "workhorses" for the process industries are types 304, 304L, 316 and 347. The molybdenum-bearing steel, type 316, is considerably better than type 304 (2). The addition of molybdenum to the austenitic alloy provides better corrosion resistance and improved resistance to pitting.

Localized Corrosion

Corrosion is the deterioration that occurs when a metal reacts with its environment. Corrosion is either uniform, and the metal corrodes at a similar rate over its entire surface, or it is localized, in which case the corrosion occurs at one part of a metal surface at much higher rate than over the rest of the surface. Different alloys, for example stainless steels, are affected to different degrees, and localized attack takes many different forms. Various forms of localized corrosion include: pitting corrosion, crevice corrosion, stress corrosion

cracking and intergranular corrosion. Pitting and crevice corrosion will be discussed in detail. Localized corrosion may occur on most metals, but this research is restricted to 304 stainless steel, an alloy commonly used in practice.

Crevice Corrosion

Crevice corrosion is one type of localized corrosion process. It occurs within or adjacent to a crevice formed by contact with another piece of the same or another metal or with a nonmetallic material. Crevice corrosion is common in easily passivating alloys such as stainless steels; its unpredictability can result in difficulties when using these materials in chloride-containing environments. Crevice corrosion is the most important form of localized corrosion on stainless alloys immersed in sea water (4).

Oldfield and Sutton (5) published a detailed mathematical model, in which the various stages of crevice corrosion can be simulated, taking account of the many factors involved. In this model four stages can be distinguished for crevice attack: deoxygenation, increase of the salt and acid concentrations, depassivation, and propagation. Rosenfeld and Marshakov (6) and Bates (7) reported that crevice corrosion proceeds as above.

To illustrate the basic mechanism of crevice corrosion, Fontana and Greene (2) considered a riveted plate section of metal M immersed in aerated seawater as shown in Figure 1. The overall reactions involved are the dissolution of metal M and the reduction of oxygen to hydroxide ions. These can be depicted as:

Anode: $M \longrightarrow M^{+} + \bar{e}$

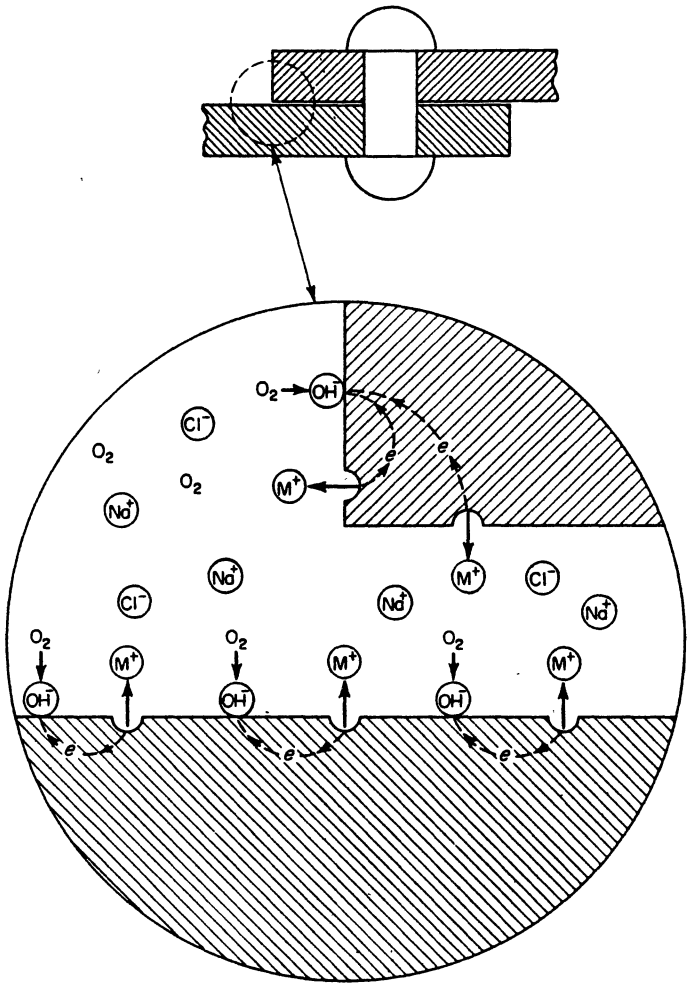

Figure 1. Crevice corrosion in aerated chloride solution, initial stage (2)

Cathode: $H_2O + 2\bar{e} + \frac{1}{2}O_2 \longrightarrow 2OH^-$

Overall Reaction: $2M + \frac{1}{2}O_2 + H_2O \longrightarrow 2MOH$

If a stainless steel crevice is placed in such a solution then this reaction initially takes place over the entire surface, inside and outside the crevice (5). Conservation of charge is maintained in both the metal and solution. If the crevice is severe enough, oxygen diffusion into it is slower than its removal by reaction on the crevice walls, and this results in the crevice solution eventually becoming deoxygenated. This is the first stage of crevice corrosion.

The dissolution of metal M continues as shown in Figure 2. This tends to produce an excess of positive charge in the solution (M^+) which is necessarily balanced by the migration of chloride ions into the crevice. This results in an increased concentration of metal chloride within the crevice. Changes now occur in the crevice solution as the metal cations from the alloy pass into solution and hydrolyze according to the equation:

$$M^+Cl^- + H_2O \rightleftharpoons MOH\downarrow + H^+Cl^-$$

Precipitation of hydroxides removes OH^- ions from the solution and reduces the pH (8), (9).

The third stage of the process is the permanent breakdown of the passive film and the onset of rapid corrosion; this occurs when the crevice solution becomes sufficiently aggressive to destroy the alloy's protective "passive" film inside the crevice.

The fourth stage is the propagation of crevice corrosion, namely, the rapid dissolution of the alloy inside the crevice and, depending on

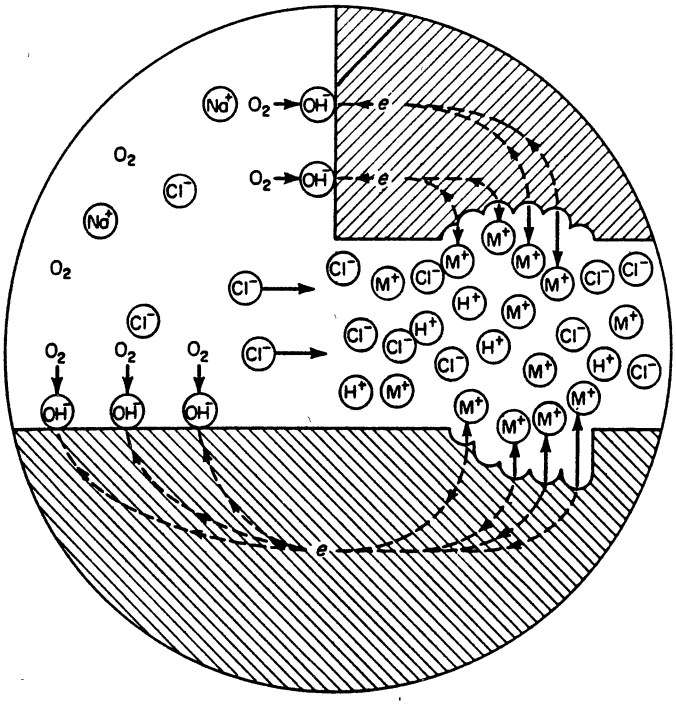

Figure 2. Crevice corrosion in aerated chloride solution, later stage (2)

conditions, perhaps some hydrogen evolution inside the crevice. This type of attack occurs in many media, although it is usually most intense in chloride solutions.

Szklarska-Smialowska and Mankowski (10) concluded that the crevice corrosion of stainless steels in NaCl solution starts inside of crevices in form of pits and can therefore be considered as a special kind of pitting corrosion.

Pitting Corrosion

Pitting corrosion, which is a further form of localized corrosion, is perhaps the most destructive and insidious form of corrosion. It is probably responsible for more unexpected plant equipment failures than any other form of corrosion (3). Pitting is recognized by the presence of pits or holes in the metal. Generally, a pit may be described as a cavity or hole with the surface diameter about the same or less than the depth (11). Pitting causes equipment to fail because of perforation with only a small percent weight loss of entire structure. Because of the small size of pits and because pits frequently remain covered with corrosion products, pit growth can proceed without being noticed until total failure occurs.

It has now been established that the occurrence of pitting requires the presence of aggressive anions like chloride, bromide or iodide in the environment (11). Some interesting observations on pitting reported by Roy (11) are:

(a) Stagnant solutions tend to cause more severe pitting than the flowing ones.

(b) Pitting occurs mainly during the shutdown period, but no damage occurs if the equipment is in continuous operation.

(c) Pits usully tend to grow in the direction of gravity. Most pits develop and grow downwards from horizontal surfaces.

(d) Pitting usually requires an extended initiation period before visible pits appear.

(e) Pits tend to occur on well polished surfaces.

There are two stages of pitting corrosion:

(a) Nucleation of active sites on the passive metal surface.

(b) Development of pits.

A corrosion pit is a unique type of anodic reaction. The pit grows by an autocatalytic process as shown in Figure 3 (2), which shows a growing pit on a metal M in aerated NaCl solution. It is called an autocatalytic process because the corrosion processes going on in a pit produce conditions which are both stimulating and necessary for the continuing activity of the pit (2). Rapid dissolution of M occurs within the pit, while oxygen reduction takes place on adjacent surfaces. These can be depicted as:

$$M \longrightarrow M^{+} + \bar{e}$$

$$O_2 + 2H_2O + 4\bar{e} \longrightarrow 4OH^{-}$$

In order to maintain electroneutrality, the rapid dissolution of metal inside the pit produces an excess positive charge in this region resulting in the migration of chloride ions into the pit. Thus there is a high concentration of $M^{+}Cl^{-}$ inside the pit. This process is self stimulating and self-propagating. Hydrolysis of $M^{+}Cl^{-}$ produces high H^{+} ion concentrations inside the pit as follows (10):

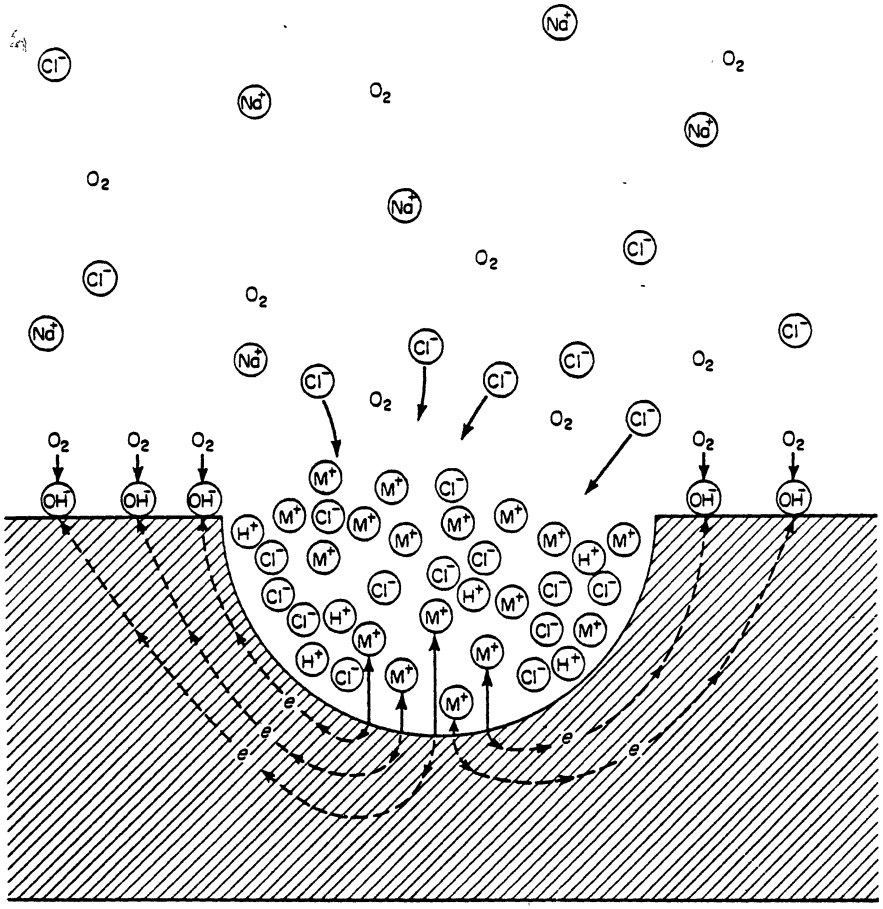

Figure 3. Autocatalytic process occuring in a corrosion pit (2)

$$M^{+}Cl^{-} + H_2O \rightleftharpoons MOH + MOH + H^{+} + Cl^{-}$$

Both hydrogen and chloride ions stimulate the dissolution of metals and alloys, and the entire process accelerates with time. The nucleation of pits is a function of the electrode potential and chloride ion concentration.

Szklarska-Smialowska (12) in her review of literature of pitting corrosion summarized the most important results and conslusions drawn by different authors on pitting research. The major area of research studied were:

1. Investigations aiming at a precise determination of the breakdown potential by different electrochemical methods.
2. Studies of the effect of alloying elements on pitting.
3. Studies of the effect of electrolyte composition.
4. Studies of the effect of different factors such as temperature, pH, cold working, heat treatment etc.
5. Measurements of the induction time for pit formation.
6. Micrographic examination, using either optical or electronic instrumentation, of metal sites most susceptible to pitting.
7. Studies of the shape of pits.
8. Studies of the kinetics of pit growth under potentiostatic and galvanostatic conditions.
9. Investigations concerning the properties of oxide films, structure, thickness and conductivity.

Potential-pH Diagrams

Most metals exist in their natural state as compounds (oxides, sulfides, etc). This is their thermodynamically stable state. Thermodynamic stability is determined not only by the given metal, but also by the corrosive medium.

The applications of thermodynamics to corrosion have been studied by means of potential-pH diagrams. There are frequently called Pourbaix diagrams after Dr. M. Pourbaix. A potential-pH diagram for iron in water proposed by Pourbaix (13) is shown in Figure 4. These diagrams are used to predict the spontaneous direction of reactions, estimate the composition of corrosion products and predict environmental changes which will prevent or reduce corrosive attack.

The potential-pH diagram is divided into three regions:

1. Immunity - the pure metal is thermodynamically stable and corrosion cannot occur;
2. Corrosion - ions of the metal are thermodynamically stable and corrosion may occur;
3. Passivity - a region where a compound of the metal is thermodynamically stable. This passive region may or may not be protective depending on the nature of the film formed.

Each line in the Pourbaix diagram relates to some equilibrium process (14). The horizontal line (a) in Figure 4 indicates potentials for the equilibrium reaction:

$$Fe \longrightarrow Fe^{2+} + 2\bar{e}$$

Iron cannot corrode below this line. This line separates the region of thermodynamic stability of iron from the corrosive region. Line (b) (Figure 4) relates the equilibrium between the ions of divalent iron in solution and solid ferric oxide:

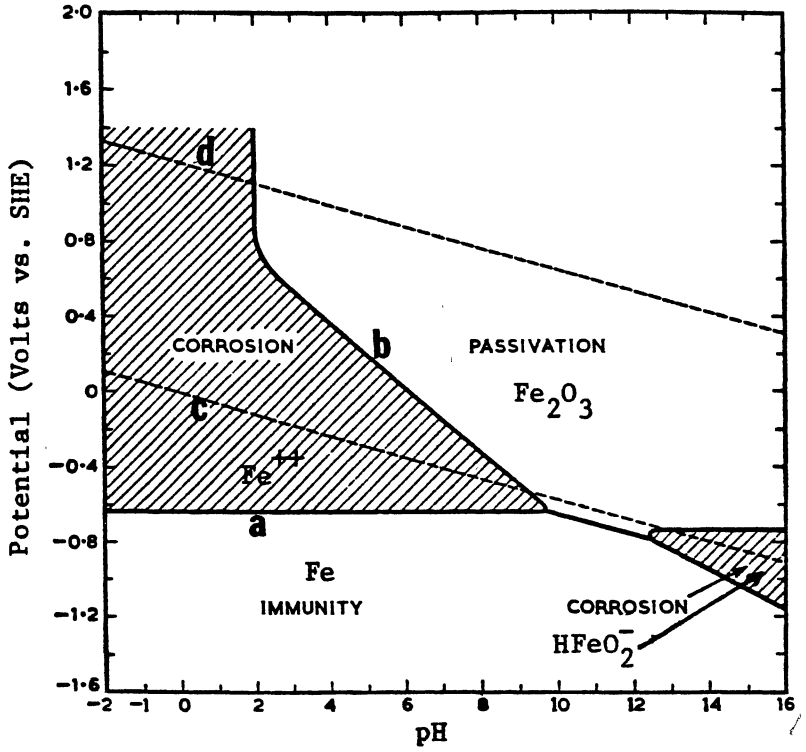

Figure 4. Simplified Potential - pH diagram for the Fe/H_2O System (13).
Temperature = 25°C

$$2Fe^{2+} + 3H_2O \rightleftharpoons Fe_2O_3 + 6H^+ + 2\bar{e}$$

This line reflects conditions for the formation of solid insoluble corrosion products in equilibrium with Fe^{2+}. Above the indicated line is the passivity region.

Iron ferrates ($HFeO_2^-$) are formed in strongly alkaline conditions in the smaller corrosion region located at the right edge. The two sloping dotted lines (c) and (d) respectively represent the equilibrium

$$H^+ + \bar{e} \rightleftharpoons \tfrac{1}{2}H_2$$

and

$$\tfrac{1}{2}O_2 + 2\bar{e} + H_2O \rightleftharpoons 2OH^-.$$

These two lines define the region of thermodynamic stability for water.

Limitations of Thermodynamic Diagrams

Limitations of thermodynamically calculated potential-pH diagrams include the following:

1. Thermodynamics cannot be used to develop potential -pH diagrams for alloys.
2. They cannot predict which of several possible species is most likely to form.
3. They cannot be used to predict the kinetics of electrode reactions (or corrosion rate).
4. They cannot predict the effectiveness of passive films which form on electrode surfaces.

These limitations led Pourbaix and other researchers to attempt to develop experimental potential-pH diagrams.

Electrochemical potential monitoring and anodic protection are areas of practical corrosion control which could benefit from the

potential-pH diagrams for alloys if they were available. Process equipment, heat exchangers and other complicated structures fail by crevice corrosion. Crevices are very hard to inspect and various laboratory studies have attempted to describe the potential and the environment inside a crevice, but these parameters cannot be measured in actual operating equipments. Thus the external measurement of potential and of environmental parameters such as temperature and pH are the only available methods for determining whether operating equipment is subject to crevice corrosion. The lack of a well-defined protection potential has prevented the refining and process industries from adopting this approach.

If we had reliable potential-pH diagrams, then corrosion inhibitors could be coupled to automatic feed systems which add new inhibitors to process streams as the inhibitor became diluted or otherwise lost its effectiveness.

Anodic protection is a means of corrosion control which relies on a protective passive film (15). Anodic protection equipment must be operated in the passive potential region to be effective. It must also maintain potentials below the protection potential to avoid pitting and crevice corrosion. The lack of well defined protection potentials has limited widespread use of anodic protection in situations where anodic protection could offer significant advantages in so far as cost benefits and reliability are concerned.

Electrochemical Techniques for Determining Protection Potential

Verink, Pourbaix and co-workers (16) identified the protection potential (E_p) using a method they termed "the electrochemical hysteresis technique". Their method involves a reverse potentiodynamic scan in the active direction. During this, the reverse scan portion of the potentiodynamic polarization curve method, the current density approaches zero. The potential where the anodic current becomes zero is defined as "the protection potential". Above this potential, pitting and crevice corrosion will occur if the nucleation site is already present, below that, corrosion will not occur.

Figure 5 shows the short term potentiodynamic polarization curve of an active-passive metal (3). When a specimen is in contact with a corrosive liquid and the specimen is unconnected to any instrumentation, the specimen assumes a potential relative to a reference electrode termed the corrosion potential, E_{corr}. The corrosion potential is also called the "steady state" or "rest" potential (17). A specimen at E_{corr} has both anodic and cathodic currents present on its surface. The current density at E_{corr} is called the corrosion current density, i_{corr}, and is a measure of the corrosion rate. The region below E_{corr} is called the cathodic region, and in this region the metal is immune to corrosion. The measured current ceases to increase with applied potential, and at a potential usually called Epp, the primary passivation potential, it begins to decrease. The beginning of this decrease is known as the active-passive transition.

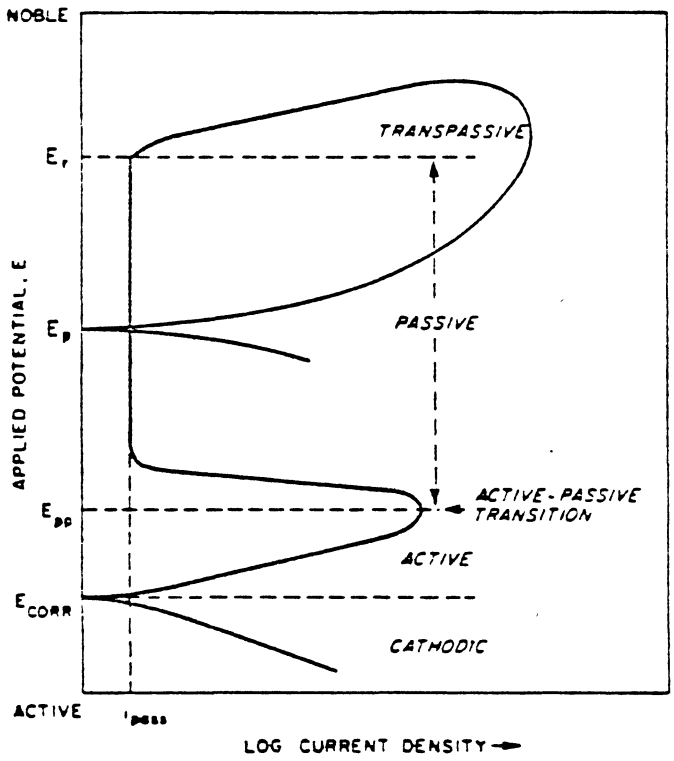

Figure 5. Idealized Polarization curve modified to include the Electrochemical Hysteresis loop (3)

The region between E_{pp} and E_{corr} is called the active region, and this is the region in which the metal specimen corrodes as the applied potential is made more positive.

Increasing the applied potential in the noble direction, another potential will be reached at which the measured current will again begin to increase. This is called the rupture potential, E_r, sometimes referred to as the "pitting potential" or "critical potential for pit intiation" (18). E_r can be defined as the potential above which the passivating film becomes locally nonprotective leading to pitting. After some time, the potential scan direction is reversed and the potential is brought down until the current density approaches zero. The electrochemical technique defines the protection potential as that potential where the current density approaches zero. In the region from E_p to E_r, according to Pourbaix and Verink (16), crevices will grow, pits will continue to grow but pits will not initiate. Below E_p, pits and crevices cannot initiate.

The passive region is the portion of the anodic curve between E_{pp} and E_r. In this region the metal exhibits a very low corrosion rate. The transpassive region includes the range of potentials more noble than E_r.

Although most of the above regions have been accepted within the research community, the concept of protection potential still remains controversial and is the subject of continuing discussion.

Sedriks, in his review book on corrosion of stainless steels, described a second method for determining the protection potential (3). He suggested a long-term potentiostatic method of confirming the protection potential. When a sample is held at the protection

potential, the current density decays to a constant value. When held at a potential more noble than E_p, current increases due to localized corrosion and more active than E_p, current decreases due to repassivation.

Wilde (4) compared results of the potentiodynamic exposures with results of long-term exposure tests of stainless steel in sea water. He concluded that protection potential measurements relate only to the conditions necessary to repassivate a growing pit after a specific period of propagation and that E_p data cannot be used to predict the corrosion performance of alloys in sea water.

Hultiquist and Leygraf (19) introduced the "potential step" method to determine the protection potential. After immersion of the test sample for one minute in the test solution, the potential is switched to a predetermined value more active than the protection potential. The potential is increased in steps of 50 mv every two minutes. The lowest potential at which the current is found to increase within two minutes is determined to be the protection potential.

A fourth method for determining the protection potential is a modification of Hultiquist and Leygraf's potential step method (20). In this technique the sample surface is first "activated" by polarizing at a potential noble to the rupture potential determined by a potentiodynamic scan (Above E_r on Figure 5). After initiating active sites, the sample is polarized to a predetermined potential active to the protection potential. Again, every two minutes the potential is increased in steps of 50 mv, and the protection potential is determined to be the lowest potential at which the current is found to increase within two minutes.

Hubbel (20), in his thesis work, used the four experimental techniques described above to determine the protection potential of stainless steel. The potentiostatic tests were two to four hours long at elevated temperatures and one to two weeks long for the room temperature environments tested. There was lack of consistency between the four methods of determining protection potential.

Purpose

The purpose of this research was to determine the protection potential of 304 stainless steel at elevated temperatures using two electrochemical techniques. The electrochemical hysteresis technique, which involves a reverse potentiodynamic scan in the active direction, was used to identify the protection potential. The protection potential was then verified by long-term immersion of samples in different environments at fixed potentials 50 mv below or above the potentiodynamically determined value.

CHAPTER II

METHOD AND PROCEDURE

Two electrochemical techniques, the potentiodynamic and potentiostatic, were used to determine the protection potential of 304 stainless steel. The potentiostatic method provided the principal experimental basis for this investigation.

Apparatus

Potentiodynamic polarization curves were generated using an EG & G Model 350 Corrosion Measurement Console with a flat specimen holder ASTM Standard G5-82, Standard Reference Method for Making Potentiostatic and Potentiodynamic Anodic Polarization Measurements (21), and ASTM Standard G61-82, Standard Practice for Conducting Cyclic Potentiodynamic Polarization Measurements for Localized Corrosion (22), were used as guides for conducting these tests.

A diagram of the polarization cell used in this research is shown in Figure 6. The cell was constructed to allow the following items to be inserted into the solution chamber: a working electrode holder, a counter electrode, a Luggin capillary probe with a salt bridge connection to the reference electrode, an inlet and outlet of purge gas, and a thermometer. All of the items inserted into the corrosion cell were constructed of materials that would not deteriorate in the test solutions.

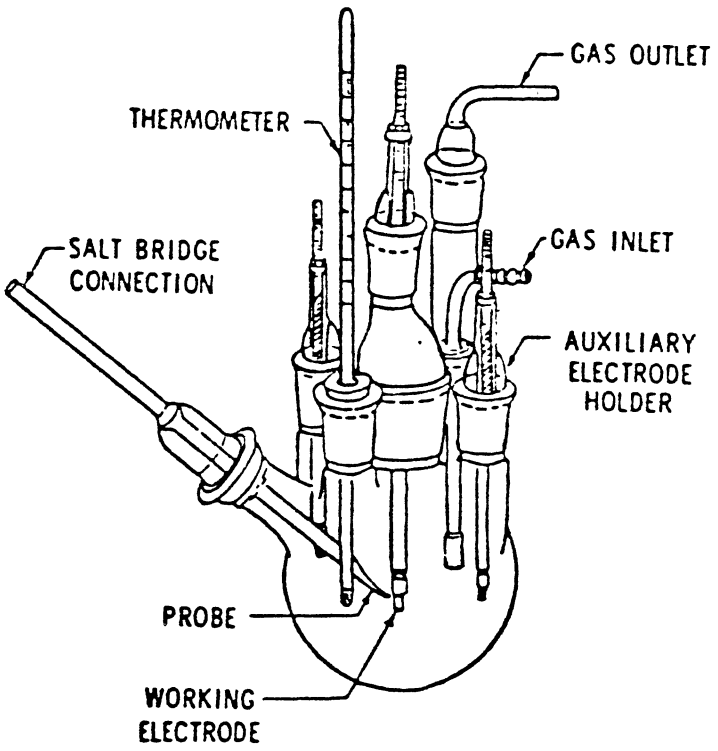

Figure 6. Schematic Diagram of Polarization Cell (21)

The Luggin probe and salt bridge were used to connect the saturated Calomel reference to the test solution. The potential of the Calomel electrode was checked at periodic intervals to ensure the accuracy of the electrode.

Counter electrodes were made by soldering platinum mesh to copper lead wires. Stop-off paint was used to insulate all but the platinum mesh from the test solution.

The thermometer was used to indicate the temperature of the electrolyte. The electrolyte temperature was maintained at $\pm 2^{o}C$ about the solution temperature with thermostatically-controlled water baths.

Two kinds of working electrode were used in this research. In the development of the potentiodynamic polarization curves, the working electrode holder shown in Figure 7 was used. The holder was designed to accept specimens of 0.625 ± 0.01 inch in diameter and up to 0.125 inch thick. The sealing washer was made of Kalrez, a new fluorocarbon elastomer with a chemical resistance approaching that of Teflon (a registered trademark of Dupont Corporation). The Kalrez washer exposes $1cm^2$ of the specimen to the test solution. The Kalrez washer is machined to minimize crevices which could affect experimental results.

For the verification of protection potentials during long-term potentiostatic exposures, the "Multiple Crevice" working electrode holder shown in Figure 8 was used. This sample holder purposely creates crevice sites. It is a modified design of the specimen holder used by Anderson (23). The stainless steel samples used in this holder were 1 inch in diameter and the exposed surface area was $9.275cm^2$ after the sample holder were assembled.

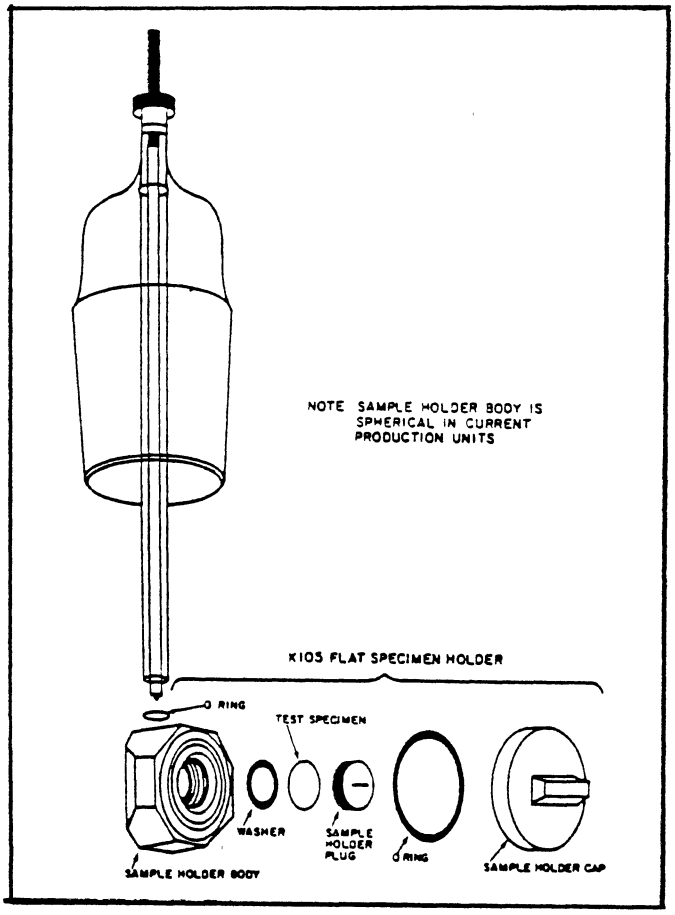

Figure 7. Exploded view of K105 flat Specimen Holder

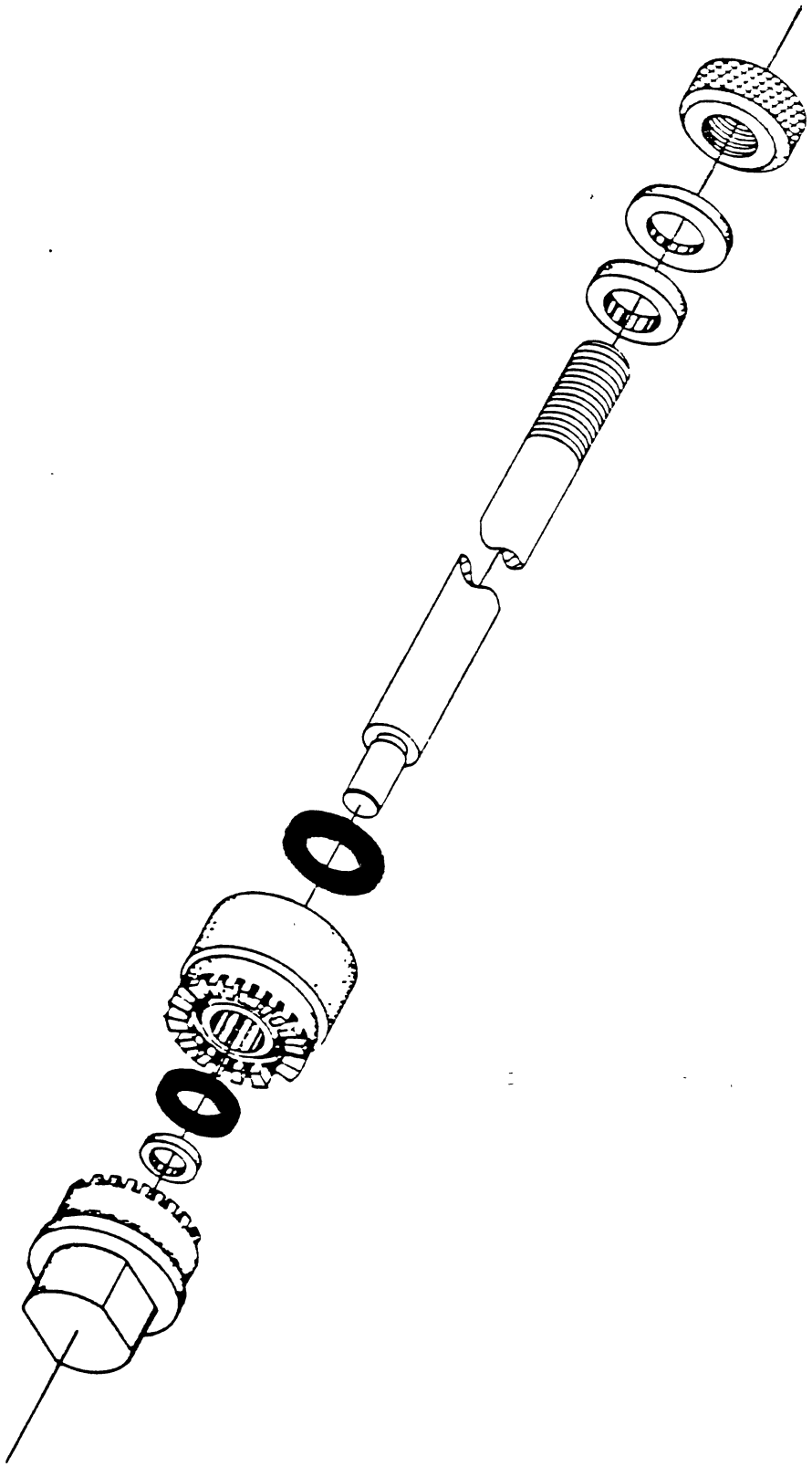

Figure 8. Multiple Crevice Assembly Working Electrode Holder.

The Wenking Potentiostat LT 73 plus our own "baby" potentiostats were also used to verify the protection potential. A simple potentiostatic circuit shown in Figure 9 was used to construct the "baby" potentiostats (24).

Experimental Procedure

Sample surfaces were prepared by wet grinding with 240-grit SiC paper, followed by wet polishing with 600-grit SiC paper until previous course scratches were removed. The specimens were washed in acetone for 15 minutes, rinsed in distilled water, and air dried before use. The samples were then mounted on the electrode holder.

The buffered electrolytes (Table II) used in this research were similar to those used by Cusumano (25), Hubbell (20) and others. Buffered solutions were used to insure that solution ions would not form complexes with the metal ions present from sample dissolution. The pH values of the test solutions were all determined at $20^{o}C$. Chloride containing media were made by adding to the known electrolyte solution a 0.1M NaCl solution. Small additions of NaOH or H_2SO_4 were used to titrate to the whole number values of 3, 5, 7, 9, 11, and 13 when deviations in pH occured due to additions of 0.10 molar NaCl. The pH was checked after each experiment to verify that the buffering capacity of the solution had not been exceeded by chemical interactions taking place during the experiment.

The solutions were purged prior to immersion of the test specimen, for a minimum of one half hour with N_2 gas to remove oxygen. The samples were transferred to the corrosion cell and salt bridge probe tip was adjusted so that it was about 2mm from the sample electrode. The

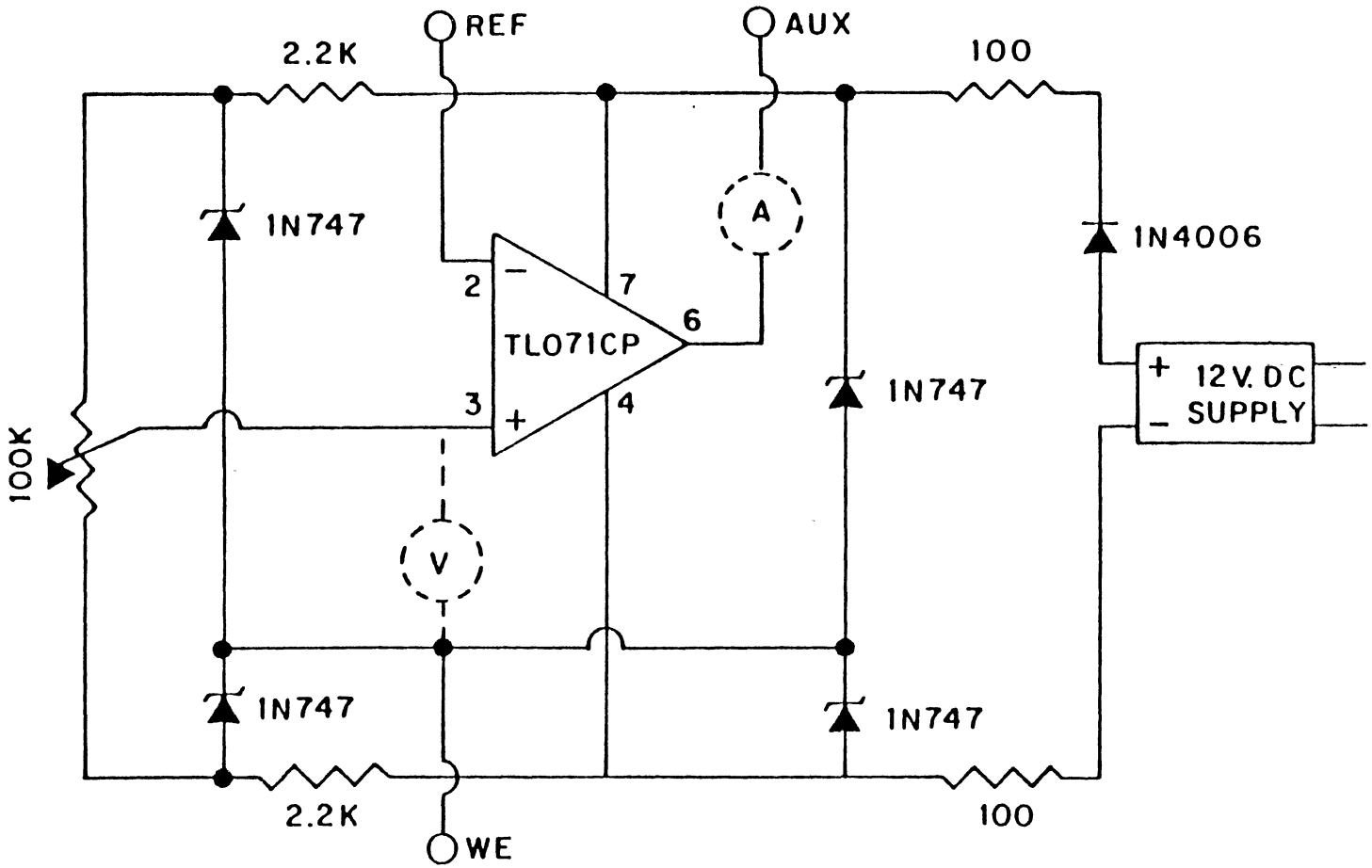

Figure 9. A Simple Potentiostatic Circuit (24)

TABLE II

ELECTROLYTES

PH	Composition
3.0	0.001M H_2SO_4 0.005M $KHC_8H_4O_4$
5.0	0.030M NaOH 0.060M $KHC_8H_4O_4$
7.0	0.046M NaOH 0.046M $KHC_8H_4O_4$
9.0	0.100M $NaHCO_3$ 0.010M NaOH
11.0	0.001M NaOH
13.0	0.10M NaOH

potential scans were started one hour after sample immersion. This allowed the samples to reach an equilibrium corrosion potential with the specific environment they were placed.

Polarization data was obtained at a scan rate of 2mV/sec or 7.2V/hr using the EG & G Model 350 Corrosion Measurement Console in the potentiodynamic mode. These fast scans were performed to determine a ball park value of E_r, the rupture potential. This value was needed to estimate a potential value at which to preprogram the return scan on the instrument. In the pitting mode, polarization data using the electrochemical hysteresis return scan method was obtained. All pitting scans were performed at a scan rate of 0.833 mV/sec, 3V/hr, the same scan rate used by Hubbel (20).

Potentiostatic exposures were performed to verify the protection potential results determined by the potentiodynamic method. The results were checked by long-term immersion of samples in environments at fixed potentials 50 mV below or above the potentiodynamically determined protection potential. The multiple crevice sample holder described earlier was used for the potentiostatic exposures. The maximum long-term exposures were one week long. The experimental set up is shown in Figure 10.

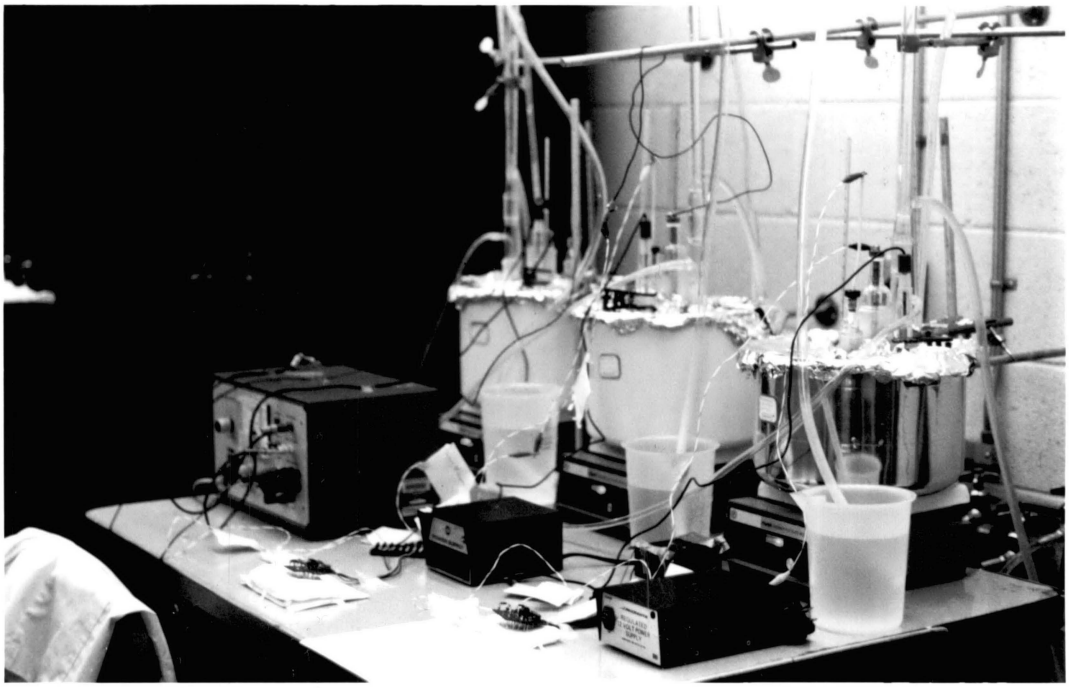

Figure 10. Experimental set up

CHAPTER III

RESULTS AND DISCUSSION

Potentiodynamic polarization curves for 304 stainless steels in deaerated nil-chloride and 0.1M NaCl electrolyte solutions are shown in Appendix A. The curves were constructed by exposing the specimen to the corrodent for one hour, followed by scanning in the noble direction and then reversing the scan in the active direction. The polarization results are summarized in Tables III and IV. These results were reproducible to $\pm$ 20 mV in replicate experiments.

Active-passive transitions were not observed on most of the potentiodynamic curves. These curves do not exhibit the peak-shaped active to passive transition because the specimen has been already fully passivated. The potentiodynamic curves exhibited several different characteristic shapes. Two types of curves were observed, one type did not exhibit a hysteresis effect such as the type shown in Figure 11(a) and one type exhibited a hysteresis effect and is shown in Figure 11(b). The hysteresis effect is strongly indicative of the tendency of the material to undergo pitting. No pit initiation and growth took place on any specimen that did not display hysteresis behavior during polarization. In some cases (Figures 22, 26, 28 -- Appendix A), the reverse scan traced the same path as the forward scan in the region beyond where the current density begins to increase very rapidly with applied potential. The specimens that produced these

TABLE III

TYPICAL POTENTIODYNAMIC POLARIZATION PARAMETERS
304 STAINLESS STEEL ALLOY

TEMPERATURE = 80°C, NIL-Cl

pH	VOLTS VS SCE Ecorr	Ep
3	-0.406	0.574
5	-0.017	0.654
7	-0.050	0.519
9	-0.334	0.403
11	-0.247	0.160
13	-0.444	-0.067

TABLE IV

TYPICAL POTENTIODYNAMIC POLARIZATION PARAMETERS FOR 304 STAINLESS STEEL ALLOY

Temperature = 80°C, 0.1 M NaCl

PH	Volts vs SCE	
	Ecorr	Ep
3	-0.422	-0.342
5	-0.256	-0.057
7	-0.374	-0.136
9	-0.590	-0.385
11	-0.700	-0.244
13	-0.210	-0.075

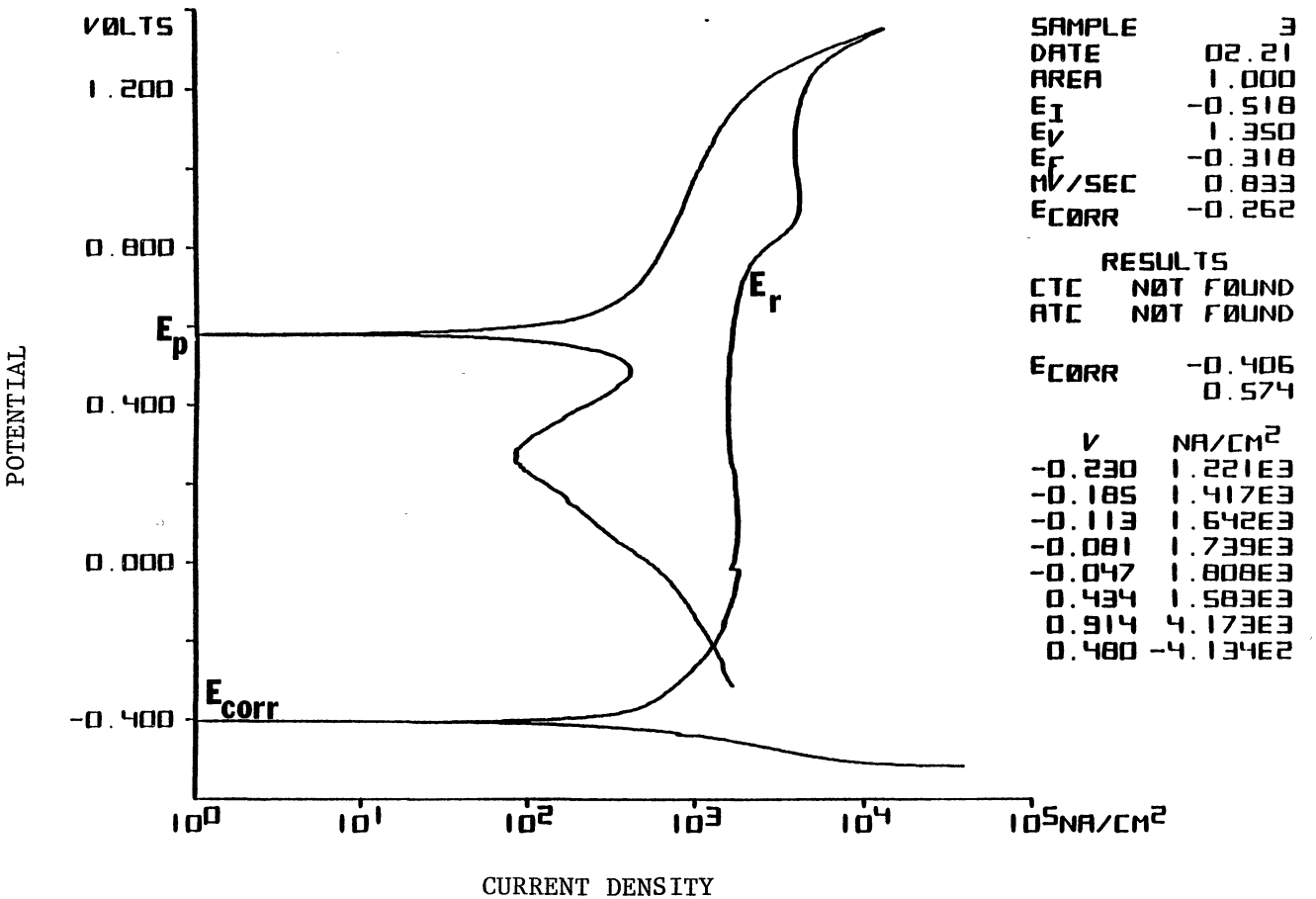

Figure 11(a) Potentiodynamic Polarization curve for 304 Alloy, pH = 3.00, Ni1-Cl^-, Temperature = 80^oC

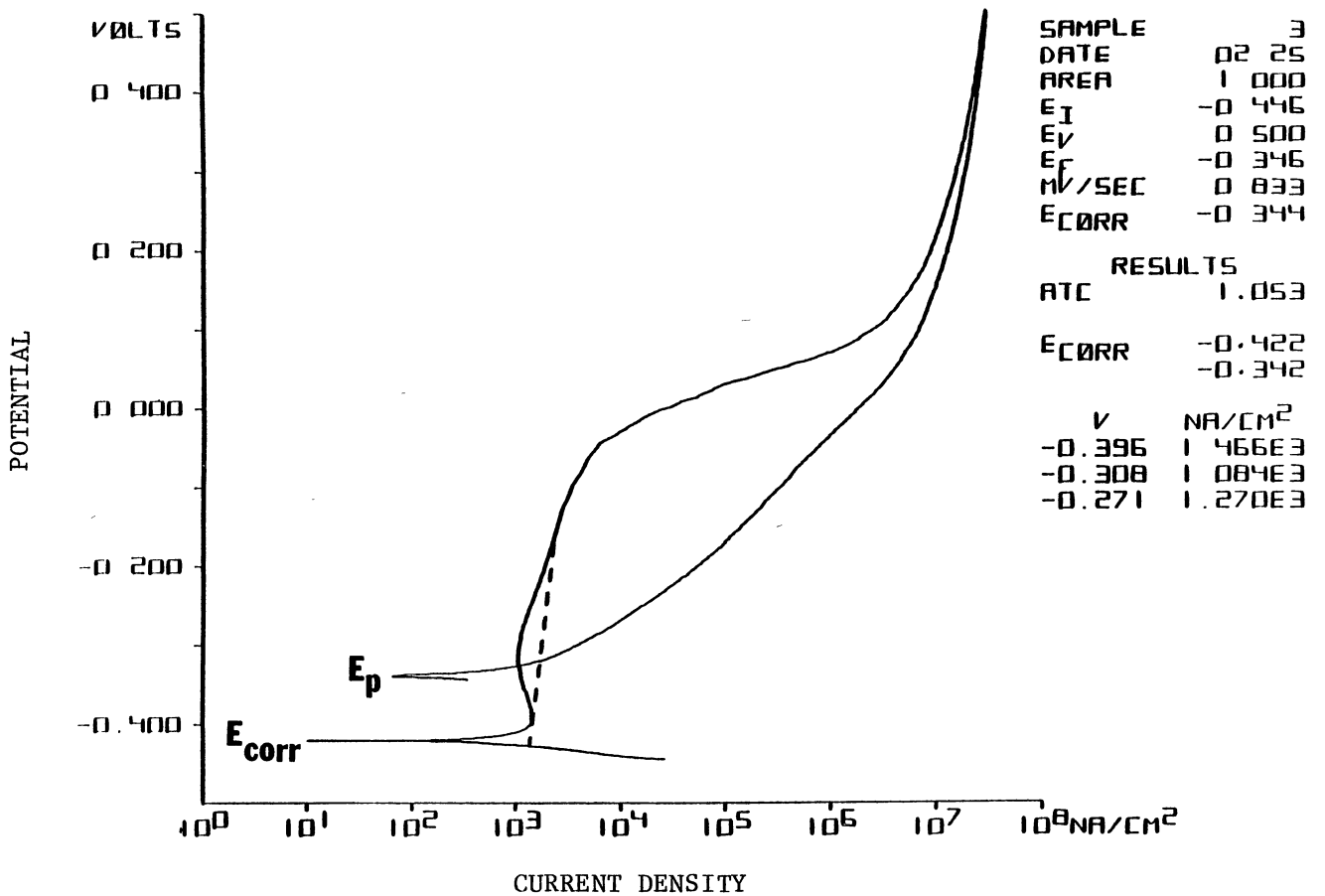

Figure 11(b) Potentiodynamic Polarization Curve for 304 Alloy, pH = 3.00, 0.1M NaCl, Temperature = 80^{o}C

curves have little tendency to pit. For samples that displayed hysteresis behavior, pitting or crevice corrosion, or both, occured. The hysteresis effect was mainly observed on samples that were immersed in chloride containing media while the nil-chloride media exhibited no hysteresis effect. A wider hysteresis loop means that 304 stainless steel has very poor resistance to corrosion in that environment (4).

Two important potentials used to characterize the hysteresis loop are E_r, the breakdown potential, (or pitting potential or rupture potential), corresponding to a point where the current begins to increase very rapidly with applied potential, and E_p, the protection potential, defined as the point where the current density approaches zero on the reverse scan. The rupture potentials were very difficult to identify on some curves.

In acidic aqueous chloride solutions, where the likelihood of pitting of stainless steels is a concern, the corrosion potential, E_{corr}, is often noble to the potential defining the active-passive transition. The anodic polarization curve, therefore, does not pick up the active-passive transition, and the experimental curves are of the types indicated by the unbroken lines in Figure 12(3). The separation of E_{corr} and E_r determines if pitting of stainless steel will occur or not in the environment being tested. If E_{corr} is close to E_r, any small change in the oxidizing power of the solution, can produce pitting by reducing the separation between E_{corr} and E_r. If E_{corr} is significantly active to E_r, as shown in Case A, of Figure 12, pitting is less likely to occur in that alloy/environment combination.

The protection potential (E_p) and rupture potential (E_r) were found to become more active as the chloride ion concentration was increased.

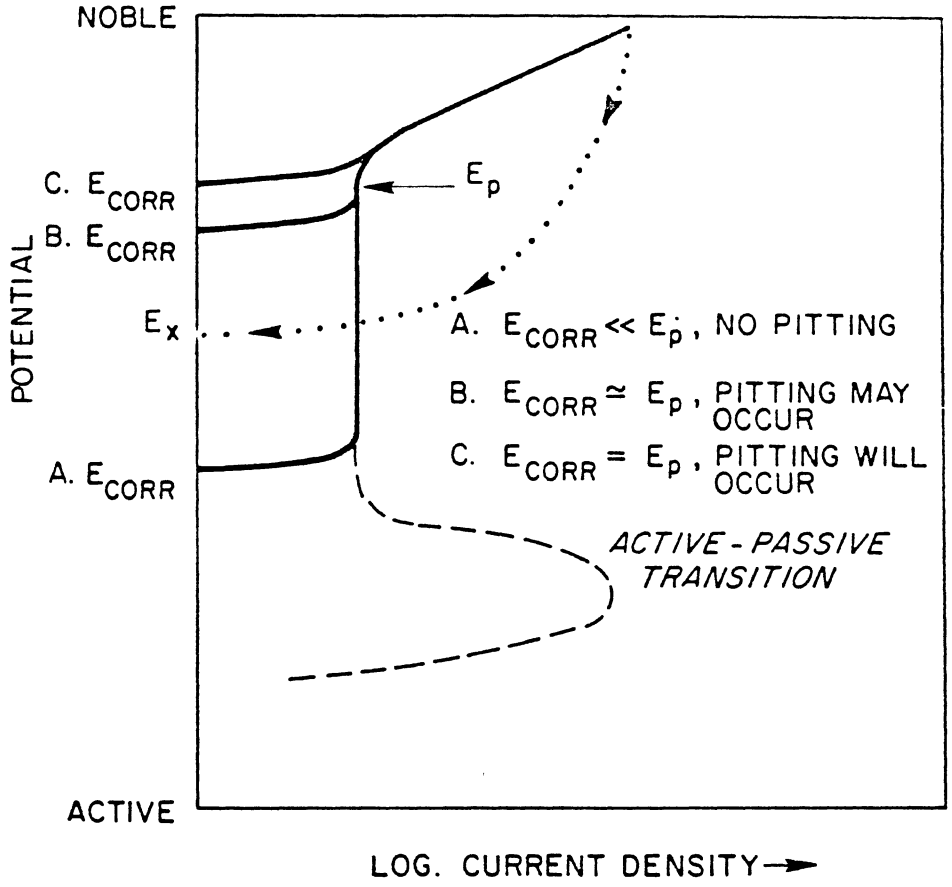

Figure 12 Schematic Polarization curve illustrating conditions under which pitting may or may not occur (3)

The pH effect on E_p or E_r was not observed.

The potentiodynamic experiments were carried out at an elevated temperature of 80°C. The effect of temperature on potentiodynamic curves was not studied. However, several researchers have found that both pitting potential and protection potential depend on temperature. Increasing the temperature generally causes the pitting potential to attain more active values which indicates an increased tendency towards pitting (3).

Protection potential (E_p) values (Table III and IV) obtained from the potentiodynamic polarization curves were verified using the potentiostatic method. The stainless steel samples were exposed for a maximum of one week in nil-chloride and chloride containing environments at potentials both active and noble to E_p determined potentiodynamically. When the sample was exposed to a potential 50 mV above E_p (determined by reversing the sweep after an arbitrary current density is reached) and no corrosion occured, additional experiments were conducted. The following experiments were raised each time by 50 mV above the previous value until crevice and/or pitting corrosion occured. The final exposure with corrosion determined E_A (potential 50 mV above E_p). When the sample was exposed to a potential 50 mV below E_p and corrosion occured, additional experiments lowering the potential by 50 mV each time were conducted. The final experiment with no corrosion determined E_B (potential 50 mV below E_p). The final values of E_p reported in Tables V and VI are the highest potentials obtained with no corrosion. Above E_p, corrosion occured. For most samples exposed in nil-chloride environments noble to E_p (at E_A), crevice corrosion initiated during that one week exposure, with no evidence of pitting corrosion. There was both pitting and crevice

TABLE V

VERIFICATION OF PROTECTION POTENTIAL --
$\pm$ 50 MV ABOVE OR BELOW E_p

Alloy 304, Temperature = 80°C, Nil-Cl^-

pH	E_p, V_{SCE}	Above	Below
3	0.624	Crevice corrosion, no pits	No corrosion
5	0.654	Crevice corrosion, no pits	No corrosion
7	0.619	Crevice corrosion, no pits	No corrosion
9	0.753	Crevice corrosion, no pits	No corrosion
11	0.210	Crevice corrosion, and a few pits	No corrosion
13	-0.067	Crevice corrosion no pits	No corrosion

*Exposed for 7 days

TABLE VI

VERIFICATION OF PROTECTION POTENTIAL --
$\pm$50 MV ABOVE OR BELOW E_p

Alloy 304, Temperature = 80°C, 0.1M NaCl

pH	Ep, V_{SCE}	COMMENTS	
		Above	Below
3	-0.292	Crevices and a few pits	No corrosion
5	-0.057	Crevices and pits	No corrosion
7	-0.086	Crevices and pits	No corrosion
9	-0.335	Severe corrosion -crevices and pits	No corrosion
11	-0.361	Crevices and pits	No corrosion
13	-0.075	Crevices and pits	No corrosion

*Exposed for 7 days

corrosion for those samples exposed in chloride containing medias at E_A (noble to E_p). The samples exposed to potential active to E_p (at E_B) did not evidence crevice or pitting corrosion after a one week exposure. These data were qualitatively reproducible in replicate experiments.

Figure 13(a) and (b) show pictures of samples of stainless steel that were exposed for one week in nil-chloride and chloride environments at $80^{o}C$. Other pictures of pitted and creviced samples are shown in Figures 14 to 18, where it is important to note that no pitting took place on most samples exposed in nil-chloride environments except for the pH = 11.00 electrolyte (Figure 13(a)) where a few pits are seen. The potential difference between E_r and E_p for the sample exposed to pH = 11.00 electrolyte with nil-Chloride is either less or equal to 50 mV. Pits initiate above E_r and this might explain why a few pits were noticed on the sample. The applied potential was below E_r for the other samples exposed in nil-chloride media, in other words the E_A value happens to fall between the rupture potential and protection potential. For the samples exposed to chloride containing media, pits and crevices were observed after the one week exposure. Addition of chloride lowers the protection potential, and therefore the difference between E_r and E_p is decreased. This decrease makes the sample less resistant to corrosion and produces pitting corrosion. The number of pits also rapidly increases with increases in chloride concentration. In some cases, severe pitting and crevice corrosion was observed on the sample.

A sample of 304 stainless steel that was run in the potentiodynamic experiment is shown in Figure 19. Pits and crevice corrosion were observed mainly on samples that were immersed in chloride containing

Figure 13(a). Photograph of 304 Stainless Steel exposed for 7 days in nil-Cl^- Solution, Temp. = 80^oC

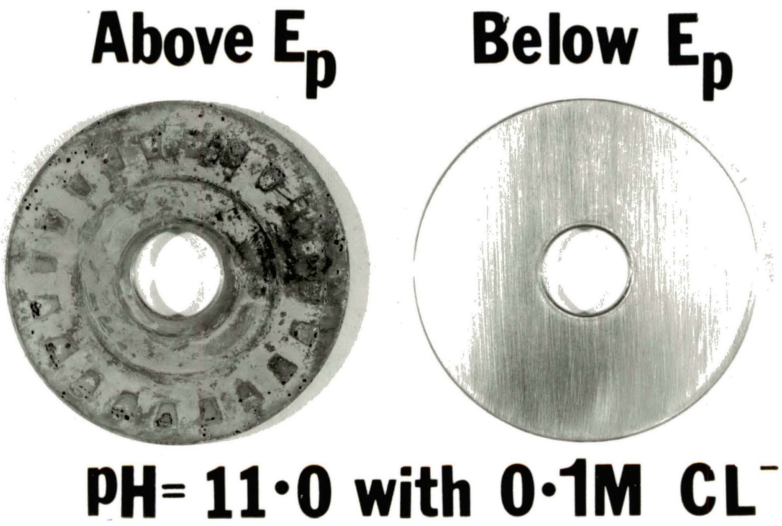

Figure 13 (b). Photograph of 304 Stainless Steel exposed for 7 days in 0.1M NaCl Solution, Temp. = 80^oC

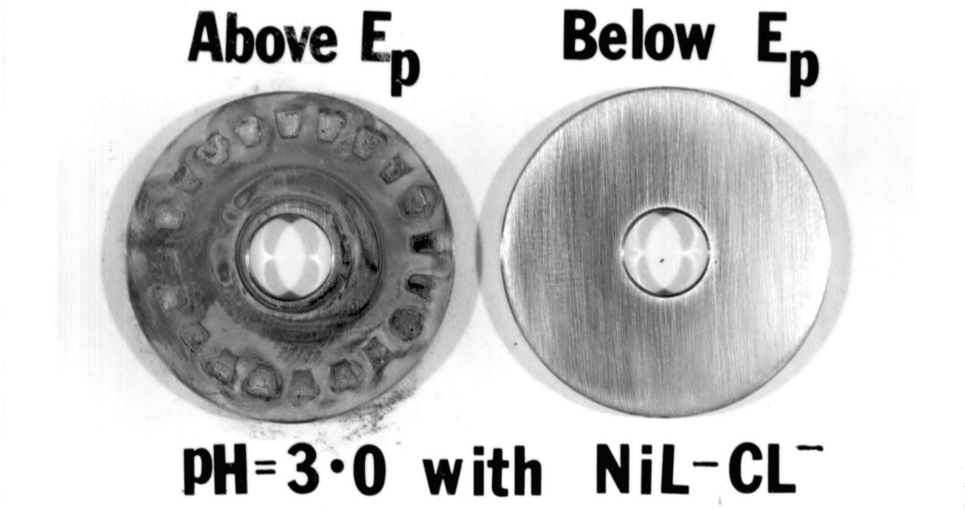

Figure 14 (a). Photograph of 304 Stainless Steel exposed for 7 days in nil-Cl Solution, Temp. = 80°C

Figure 14(b). Photograph of 304 Stainless Steel exposed for 7 days in 0.1M NaCl Solution, Temp. = 80°C

Figure 15(a). Photograph of 304 Stainless Steel exposed for 7 days in nil-Cl^- solution. Temp. = 80°C

Figure 15(b). Photograph of 304 Stainless Steel exposed for 7 days in 0.1M NaCl Solution, Temp. = 80°C

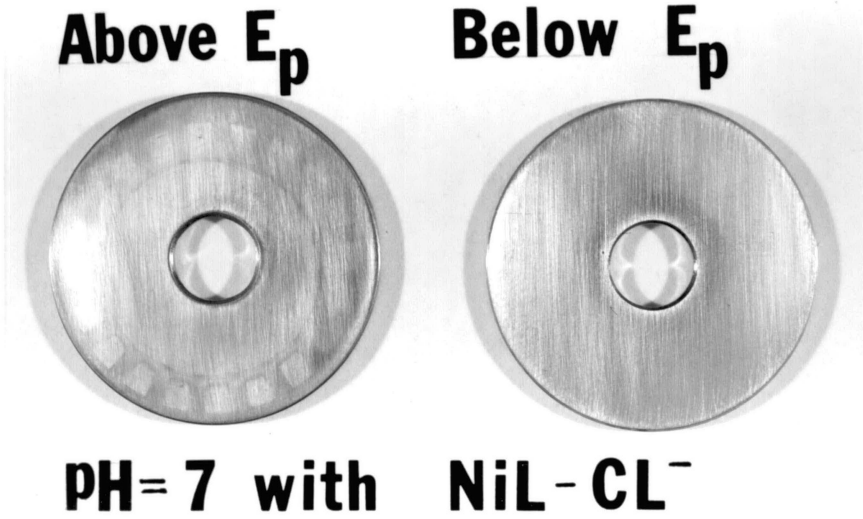

Figure 16(a). Photograph of 304 Stainless Steel exposed for 7 days in nil-Cl^- Solution. Temp. = 80°C

Figure 16(b). Photograph of 304 Stainless Steel exposed for 7 days in 0.1M NaCl Solution, Temp. = 80°C

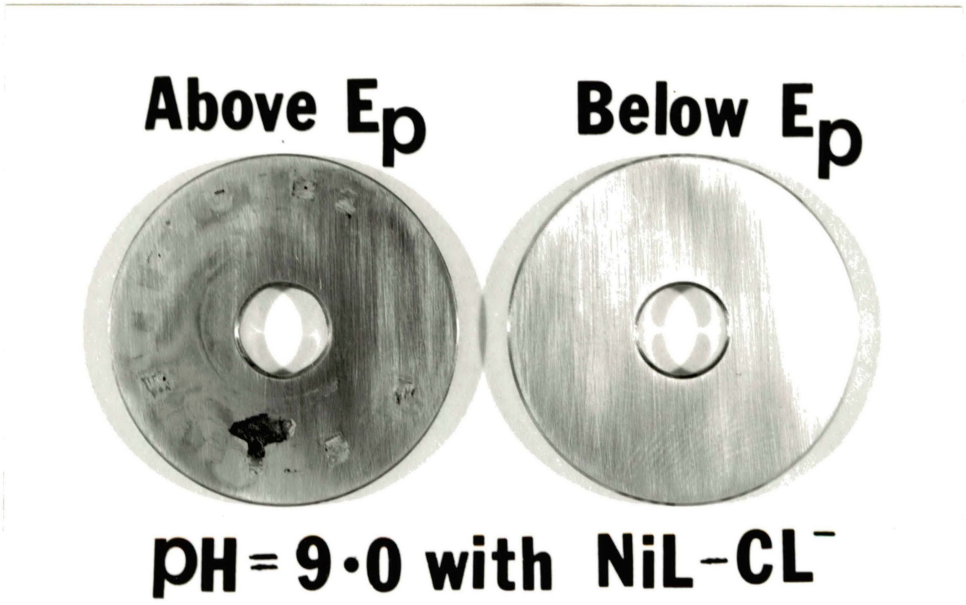

Figure 17(a). Photograph of 304 Stainless Steel exposed for 7 days in nil-Cl^- solution. Temp. = 80°C

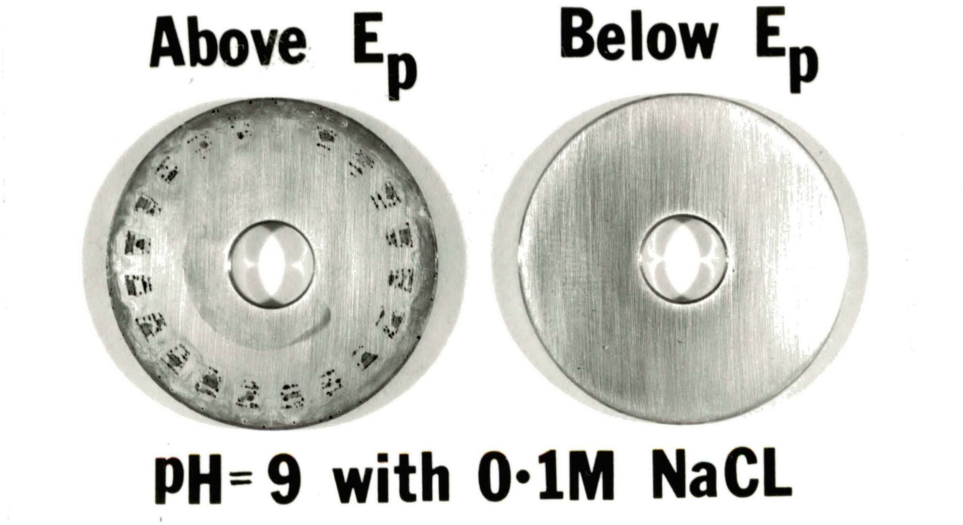

Figure 17(b). Photograph of 304 Stainless Steel exposed for 7 days in 0.1M NaCl solution, Temp. = 80°C

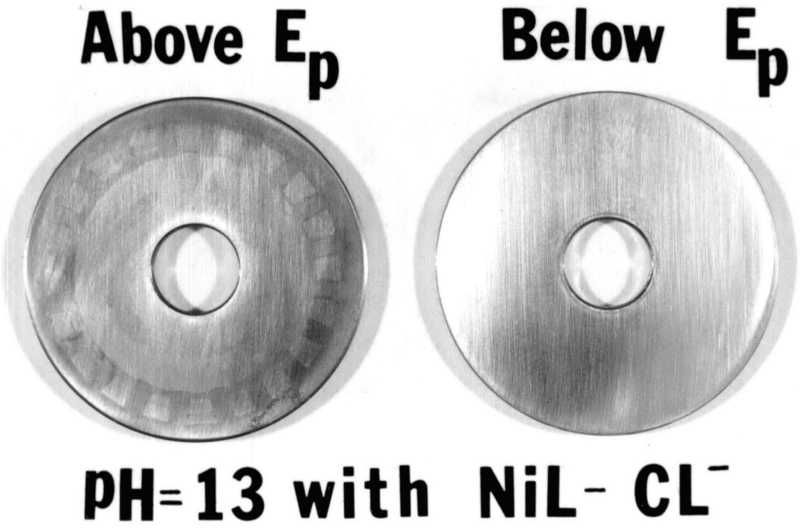

Figure 18(a). Photograph of 304 Stainless Steel exposed for 7 days in nil-Cl^- solution. Temp. = 80°C

Figure 18(b). Photograph of 304 Stainless Steel exposed for 7 days in 0.1M NaCl solution, Temp. = 80°C

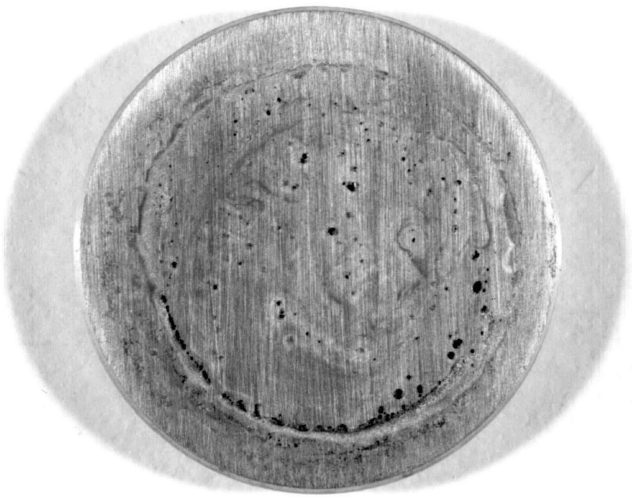

Figure 19. Photograph of Stainless Steel sample showing pitting and crevice corrosion product after 2 hour exposure using the potentiodynamic technique

media. The exposure time for this sample was two hours. Note the gasket formed crevices near to the edge of the sample.

Table VII summarizes the protection potential values obtained from the potentiodynamic and potentiostatic experiments. The protection potential was determined at 80°C in nil-chloride and chloride containing environments. Most of the results for the long-term one-week exposures are not in exact agreement with those obtained using the short-term electrochemical hysteresis method. However, the protection potentials determined from both techniques, for the environment of pH = 5 and pH = 13 with or without chloride, are in exact agreement.

Protection potential values from the potentiostatic and potentiodynamic experiments (Table VII) were used to derive the experimental potential-pH diagrams. The error on the potentiodynamic results plotted on the potential-pH diagrams has a tolerance of $\pm$ 20 mV. The potential-pH diagrams for 304 stainless steel in nil-Chloride and 0.1 M NaCl at 80°C are shown in Figure 20 and 21 respectively. The two slanted dashed lines ((a) & (b)) on the figure represent the hydrogen and oxygen evolution lines. Slopes of these lines were calculated using the Nerst equation. Sample calculations are shown in Appendix B. Most of the protection potentials for the nil-Cl electrolytes were above the oxygen evolution line (b). In this region, the electrolyte breaks down causing the water to be oxidized to oxygen. Water is thermodynamically unstable with respect to oxygen. The E_p values for the 0.1M NaCl electrolytes are in the region where water is thermodynamically stable.

The slanted and vertical line regions represent regions where 304 stainless steel is immune to corrosion using the potentiostatic and potentiodynamic methods respectively. The intersection of these two

TABLE VII

SUMMARY OF PROTECTION POTENTIAL EXPERIMENTAL RESULTS

Alloy 304, Temperature = 80°C, Nil-Cl^-

Volts vs SCE

pH	3	5	7	9	11	13
Electrochemical Hysteresis	0.574	0.654	0.519	0.403	0.160	-0.067
Long-term Potentiostatic	0.624	0.654	0.619	0.753	0.210	-0.067
Most Conservative Results	0.574	0.654	0.519	0.403	0.160	-0.067

Alloy 304, Temperature = 80°C, 0.1M NaCl

Volts vs SCE

pH	3	5	7	9	11	13
Electrochemical Hysteresis	-0.342	-0.057	-0.136	-0.385	-0.244	-0.075
Long-term Potentiostatic	-0.292	-0.057	-0.086	-0.335	-0.361	-0.075
Most Conservative Results	-0.342	-0.057	-0.136	-0.385	-0.361	-0.075

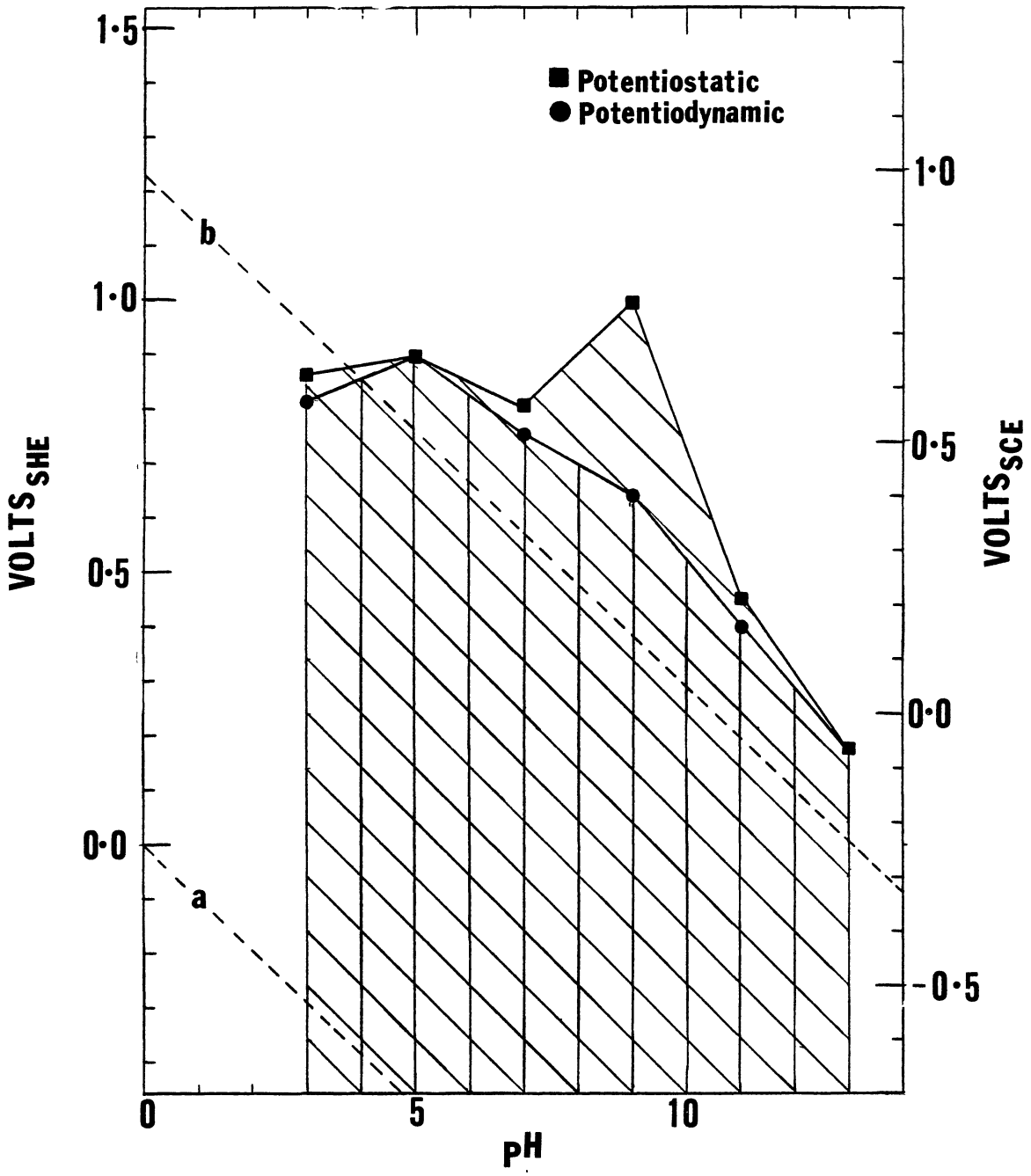

Figure 20 Experimental Potential-pH diagram of 304 stainless steel in $Nil\text{-}Cl^-$ at 80^oC

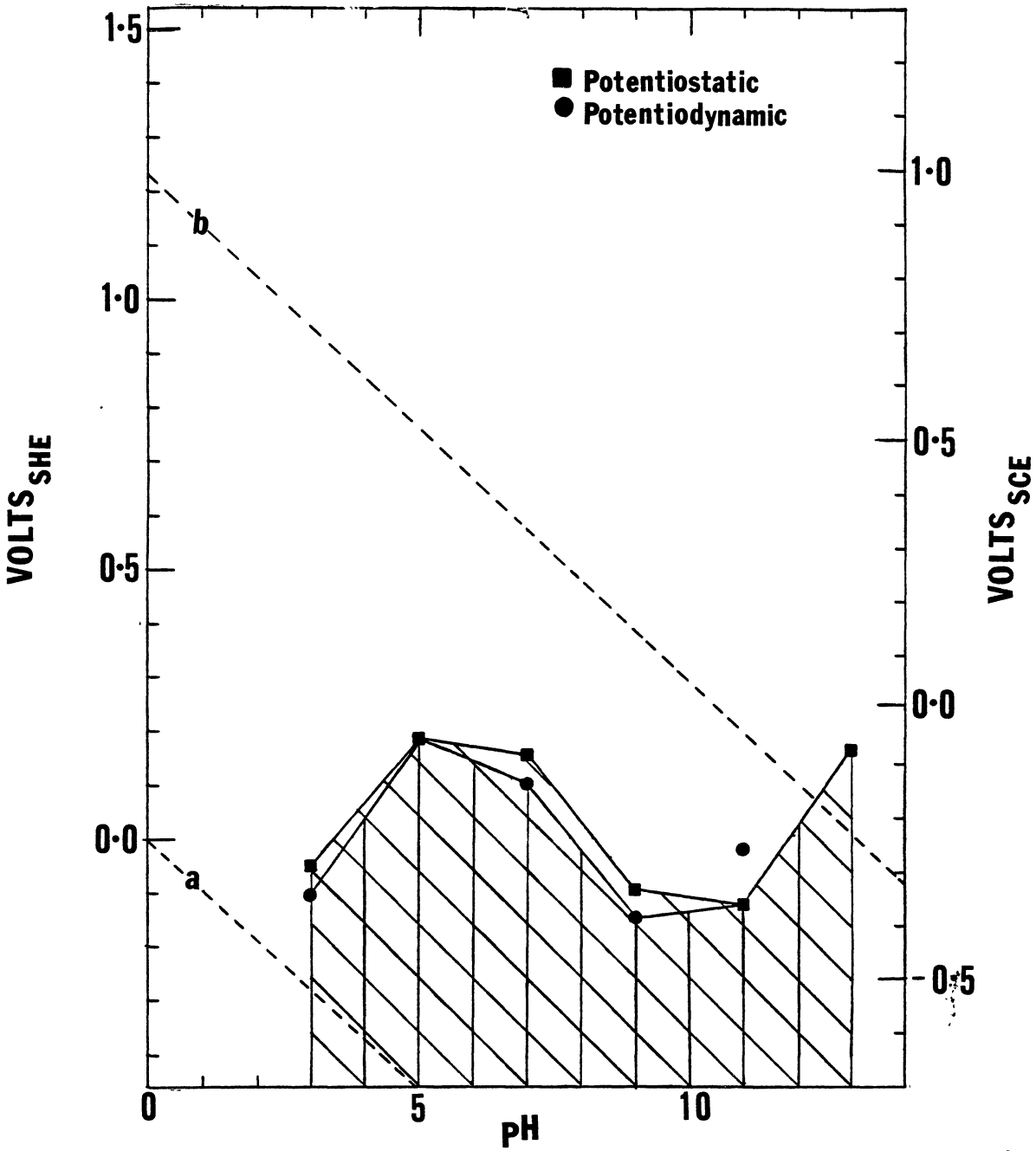

Figure 21 Experimental Potential-pH diagram of 304 stainless steel in 0.1M NaCl at 80°C

regions represent a region where 304 stainless steel should suffer negligible general corrosion and can be safely used whichever of the two methods is used. The most conservative protection potential values are reported in Table VII. The long-term potentiostatic values were less conservative compared to the short-term potentiodynamic method. This is shown in Figures 20 and 21. The reason for this cannot really be explained. The long-term method was expected to produce more conservative results. These results were compared with Hubbel's (20) results obtained after 2 hours of exposure. His short-term method also gave more conservative results than the long-term test. The protection potential values on Hubbel's diagram are higher and therefore the passivation potential region in larger. The E_p values from the long-term potentiostatic method were obtained after a long period (1 week) of exposure compared to Hubbel's (2 hours) and should be used because they correlate more with in-service test. For safety reasons, longer-term tests should be used to verify the Ep values obtained from short-term method before the E_p values can be used in industry because in some cases, such as pH = 11.00 with nil-Cl, E_p values from short-term is higher than the longer term. Addition of chloride lowered the passivation potential region.

These experimental potential-pH diagrams are reliable, and therefore we can use them for potential monitoring of an operating equipment. Long-term testing is expensive and time consuming but is necessary to predict long-term corrosion behavior.

CHAPTER IV

CONCLUSIONS

The following conclusions may be drawn from the research conducted:

1. Experimental potential-pH diagrams for 304 stainless steel are presented in Figure 20 and 21.

2. The potentiodynamic technique cannot accurately predict localized corrosion although it can provide useful screening tools for alloy evaluation.

3. Long-term potentiostatic tests are necessary to verify the protection potential determined from the short-term potentiodynamic test and these potentials are usued to develop useful potential-pH diagrams.

4. Addition of chloride lowers the protection potential. Therefore, the corrosion resistance of stainless steels is decreased in chloride environments.

5. The pH of an electrolyte was found to have very little effect on the rupture and protection potential.

6. The concept of protection potential appears to be of greater significance than the rupture potentials to industries concerned with long-term durability of complex equipment such as heat exchangers.

7. The protection potential, E_p, represents a potential that should not be exceeded if pitting and crevice corrosion is to be avoided in industrial equipments.

8. Experimental potential-pH diagrams offer a number of advantages over thermodynamically-calculated diagrams.

Suggestions for Future Work

Suggestions for further research on the topic include:

1. Narrow down the accuracy of determining the protection potential from 50 mV above or below E_p to 10 mV above or below E_p.

2. Extend the exposure times to two to four weeks.

3. Test other alloys and consider use of actual service environments.

REFERENCES

1. Payer, J., Boyd, W., Dippold, D. and Fisher, W., Materials Performanace, Vol. 19, No. 5, p. 34 (1980).

2. Fontana, M.G., Greene, N.D. Corrosion Engineering, McGraw-Hill Book Co., 1978.

3. Sedriks, A.J., Corrosion of Stainless Steels, John Wiley and Sons, New York, 1979.

4. Wilde, B.E., Corrosion Vol. 28, No. 8, p. 283-291 (1972).

5. Oldfield, J.W., Sutton, W.H. Br. Corrosion, Vol. 13, No. 1, p. 13-22 (1978).

6. Rozenfeld, I.L., Marshakov, K.I. Corrosion, Vol. 20, p. 115t-125t (1964).

7. Bates, J.F. Corrosion, Vol. 29, No. 1, p. 28-32 (1973).

8. Karlberg, G., Wranglen, G., Corrosion Science, Vol. 11, p. 499 (1971).

9. Suzuki, T., Yamabe, M., and Kitamura, Y., Corrosion Vol. 18, p. 29 (1973).

10. Szklarska-Smialowska, Z., Mankowwski, J. Corrosion Science Vol. 12, p. 925-34 (1973).

11. Roy, D.L. Corrosion and Maintenance, Vol. 2, No. 3, p. 272-276 (1979).

12. Szklarska-Smialowska, Z. Corrosion, Vol. 27,p. 223-33 (1971).

13. Shrier, L.L. Corrosion of Metals and Alloys, John Wiley and Sons, New York, 1963.

14. Tomashov, N.D., Chernova, G.P. Passivity and Protection of Metals against Corrosion, Plenum Press, New York, 1967.

15. Riggs, O., Locke, C. Anodic Protection, Plenum Press, New York, 1981.

16. Verink, E.D., Pourbaix, M. Corrosion Vol. 27, p. 495 (1971).

17. "Standard Definitions and Terms Relating to Corrosion and Corrosion Testing", A.S.T.M. Designation: G15-799, Annual book of A.S.T.M. Standards, Part 10, Metals-Physical, Mechanical, Corrosion Testing, American Society for Testing and Materials, Philadelphia, p. 827-831, 1980.

18. Pourbaix, M. Corrosion, Vol. 26, No. 18, p. 431-38 (1970) p. 431-438, (1970).

19. Huitquist, G., Leygraf, C. Materials Science and Engineering Vol. 42, p. 199-206, (1980).

20. Hubbel, M., Masters Thesis, University of Rhode Island (1982).

21. "Standard Reference Method for Making Potentiostatic and Potentiodynamic Anodic Polarization Measurements", A.S.T.M. Designation G5-78, Annual Book of A.S.T.M. Standards, Part 10, Metals -- Physical, Mechanical, Corrosion testing, American Society for Testing and Materials, Philadelphia, p. 816-826, 1980.

22. "Standard Practice for Conducting Cyclic Potentiodynamic Polarization Measurements for Localized Corrosion,", A.S.T.M. Designation G61-78, Annual Book of A.S.T.M. Standards, Part 10, Metals -- Physical, Mechanical Corrosion Testing, American Society for Testing and Materials, Philadelphia, p. 1033-1038, 1980.

23. Anderson, D. "Statistical Aspects of Crevice Corrosion in Sea Water", in Galvanaic and Pitting Corrosion - Field and Laboraatory Studies, A.S.T.M. STP 579, 1976, p. 231 (see also reference 3, Figure 5-5, page 97).

24. Simple Potentiostatic circuit designed by Texas instruments Incorporated.

22. Cusumano, R.L. Masters Thesis, University of Florida, (1971).

APPENDIXES

APPENDIX A

POLARIZATION CURVES

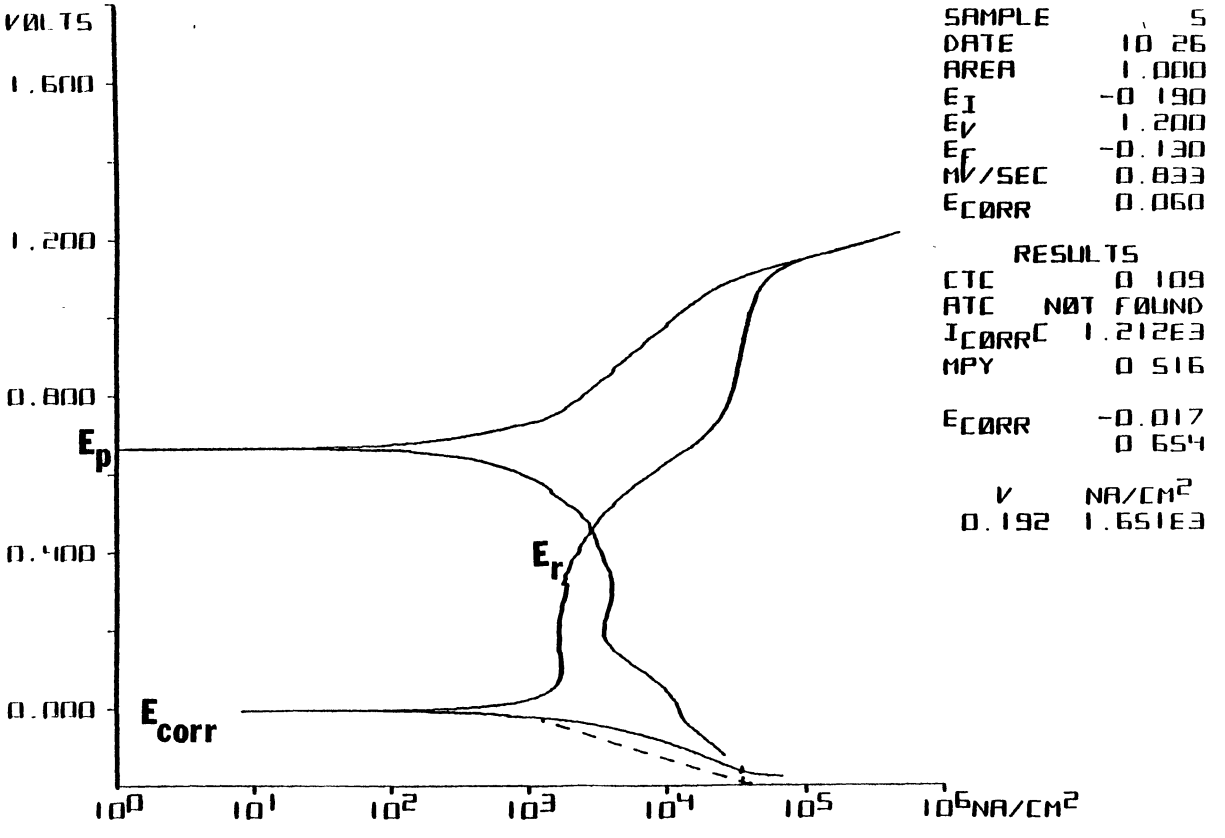

Figure 22 Potentiodynamic Polarization Curve for 304 Alloy, pH = 5.00, Nil-CL^-, Temperature = 80°C

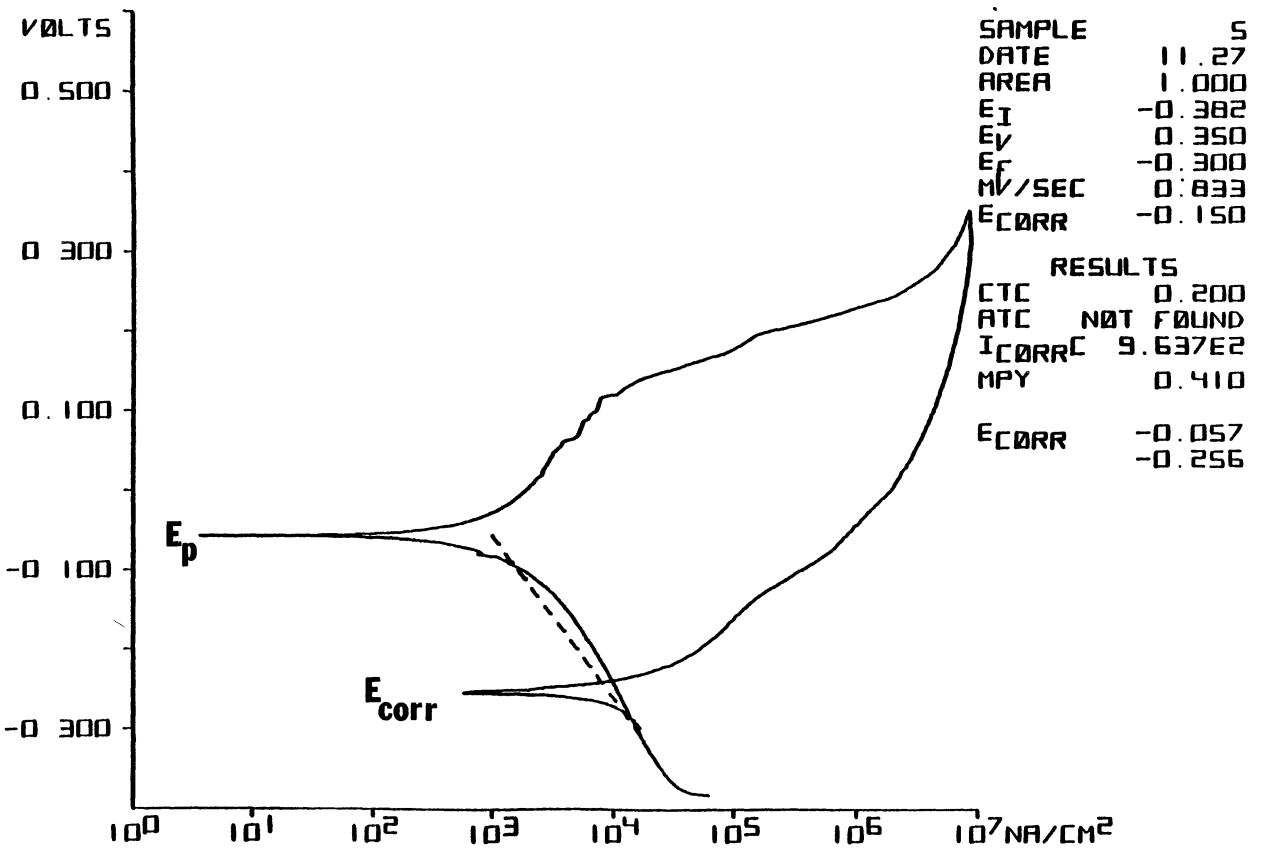

Figure 23 Potentiodynamic Polarization Curve for 304 Alloy, PH = 5.00, 0.1M NaCL, Temperature = 80°C

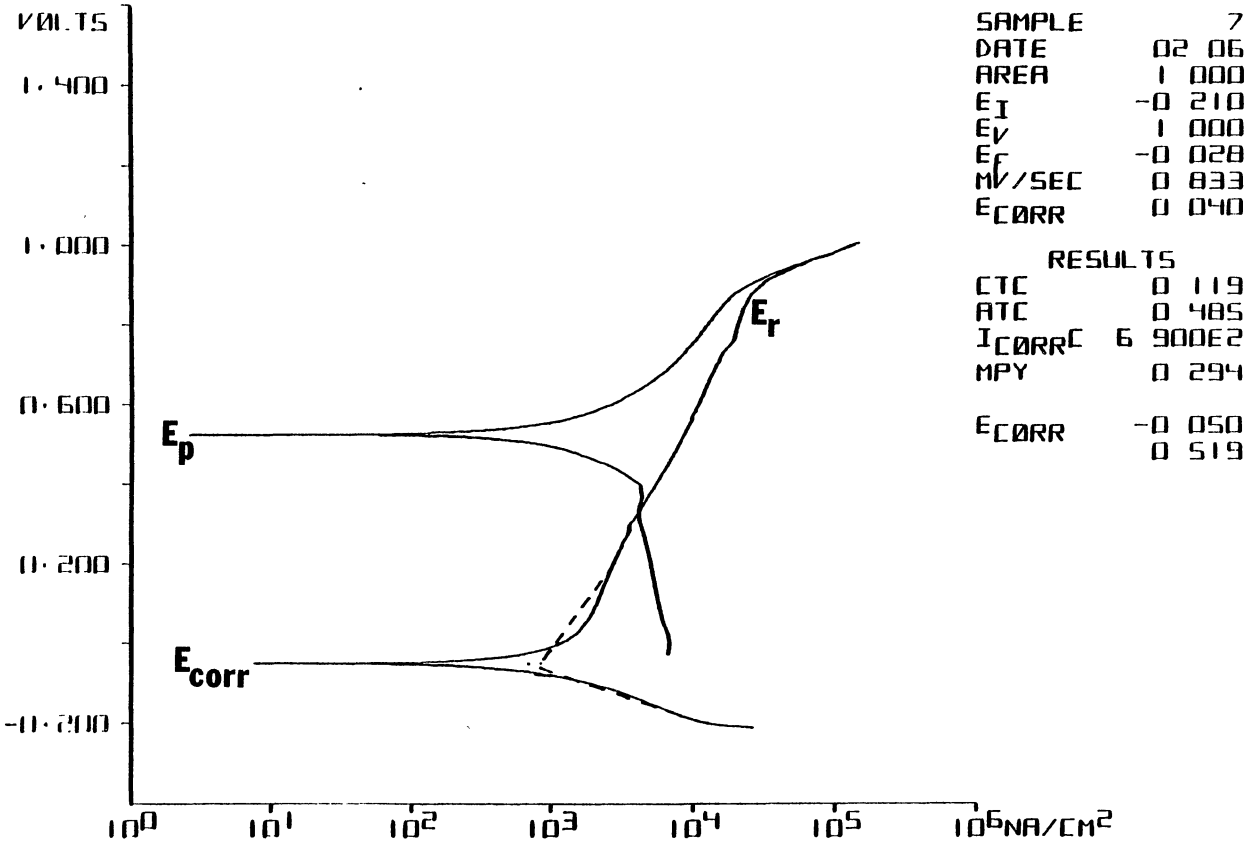

Figure 24 Potentiodynamic Polarization Curve for 304 Alloy, pH = 7.00, Nil-CL^-, Temperature = 80^oC

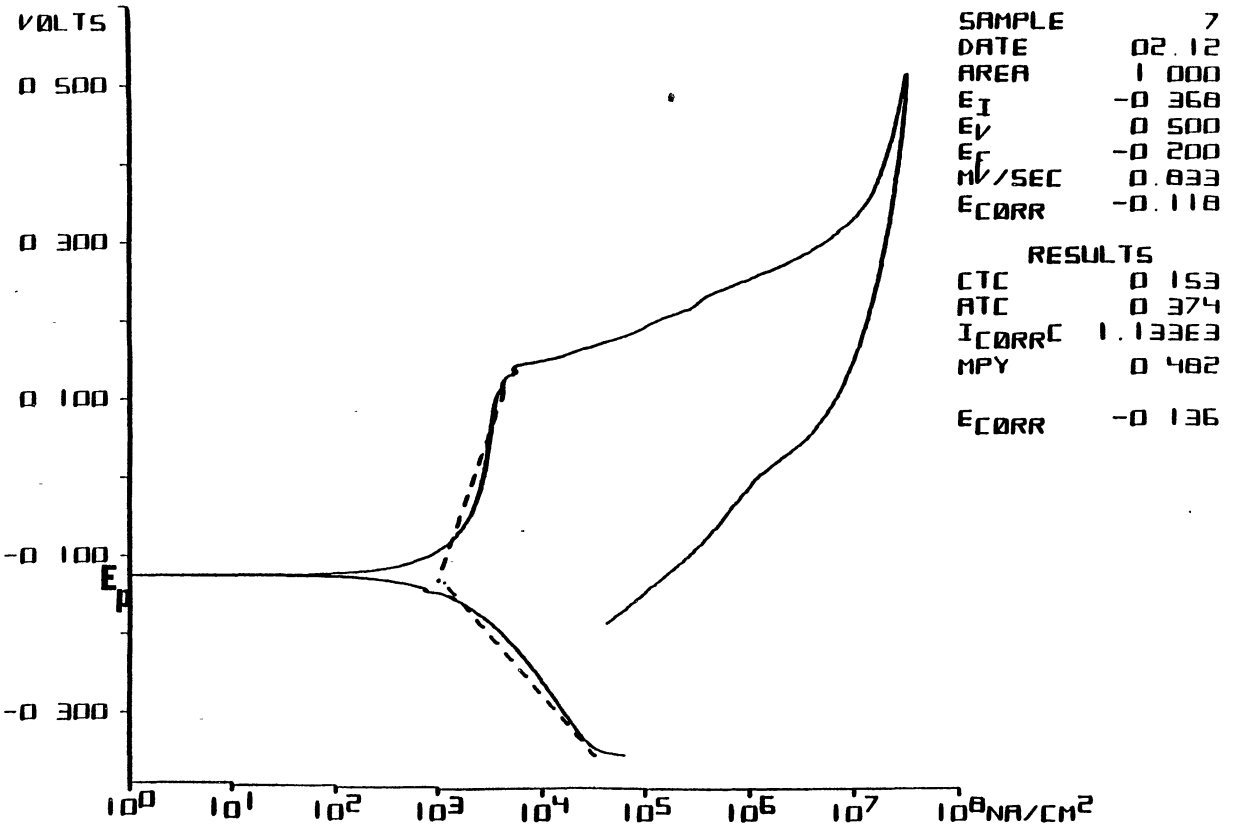

Figure 25 Potentiodynamic Polarization Curve for 304 Alloy, pH = 7.00 0.1M NaCL, Temperature = 80°C

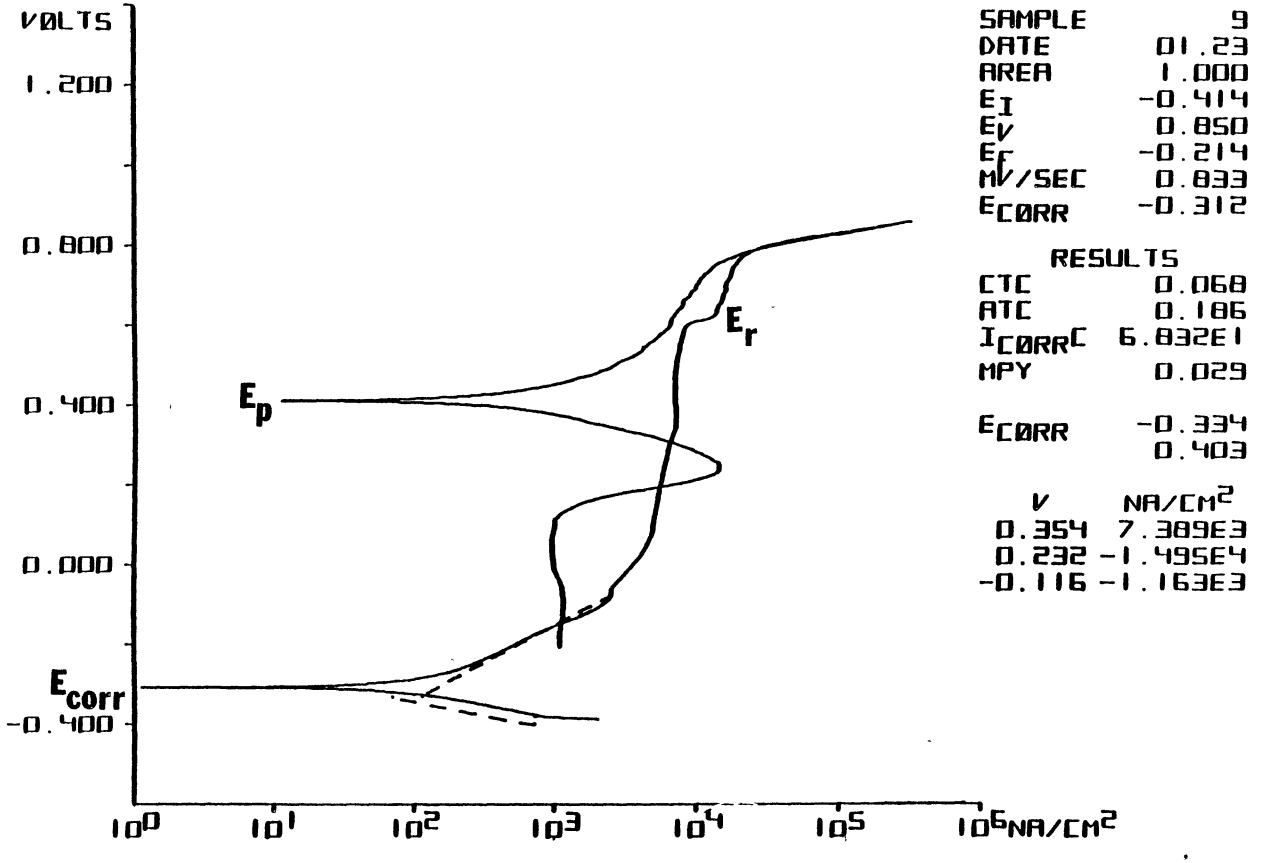

Figure 26 Potentiodynamic Polarization Curve for 304 Alloy, pH = 9.00 Nil-CL^-, Temperature 80°C

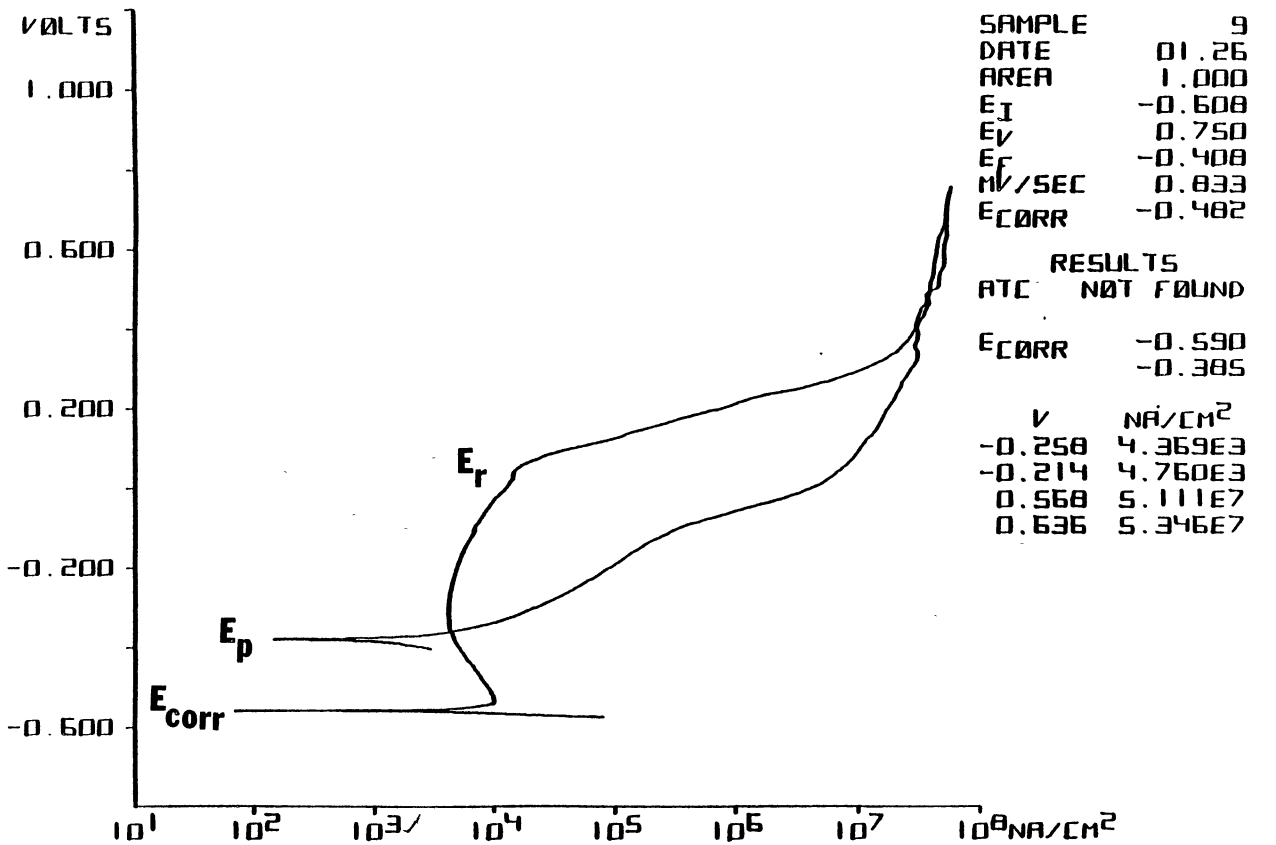

Figure 27 Potentiodynamic Polarization Curve for 304 Alloy, pH = 9.00, 0.1M NaCL, Temperature = 80°C

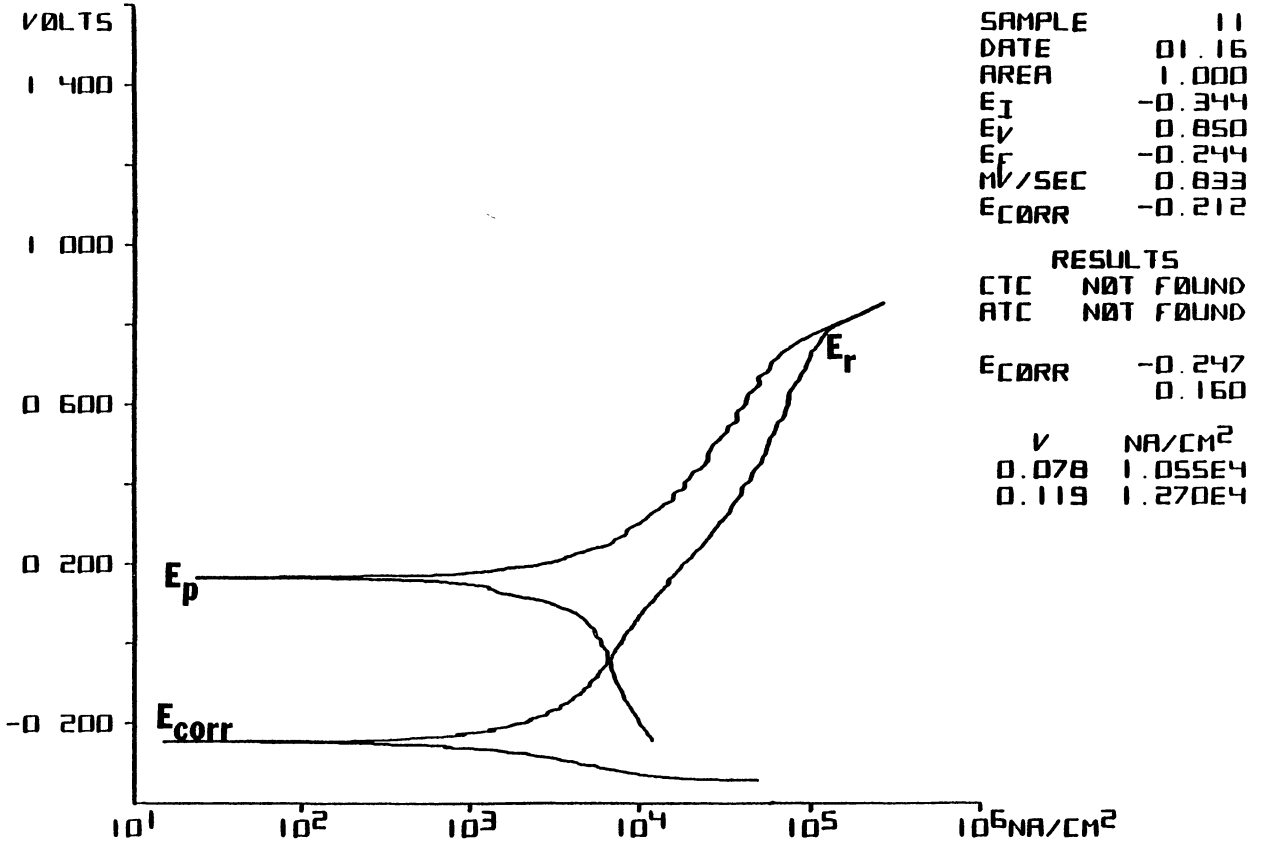

Figure 28 Potentiodynamic Polarization Curve for 304 Alloy, pH = 11.00, NiL-CL^-, Temperature = 80^oC

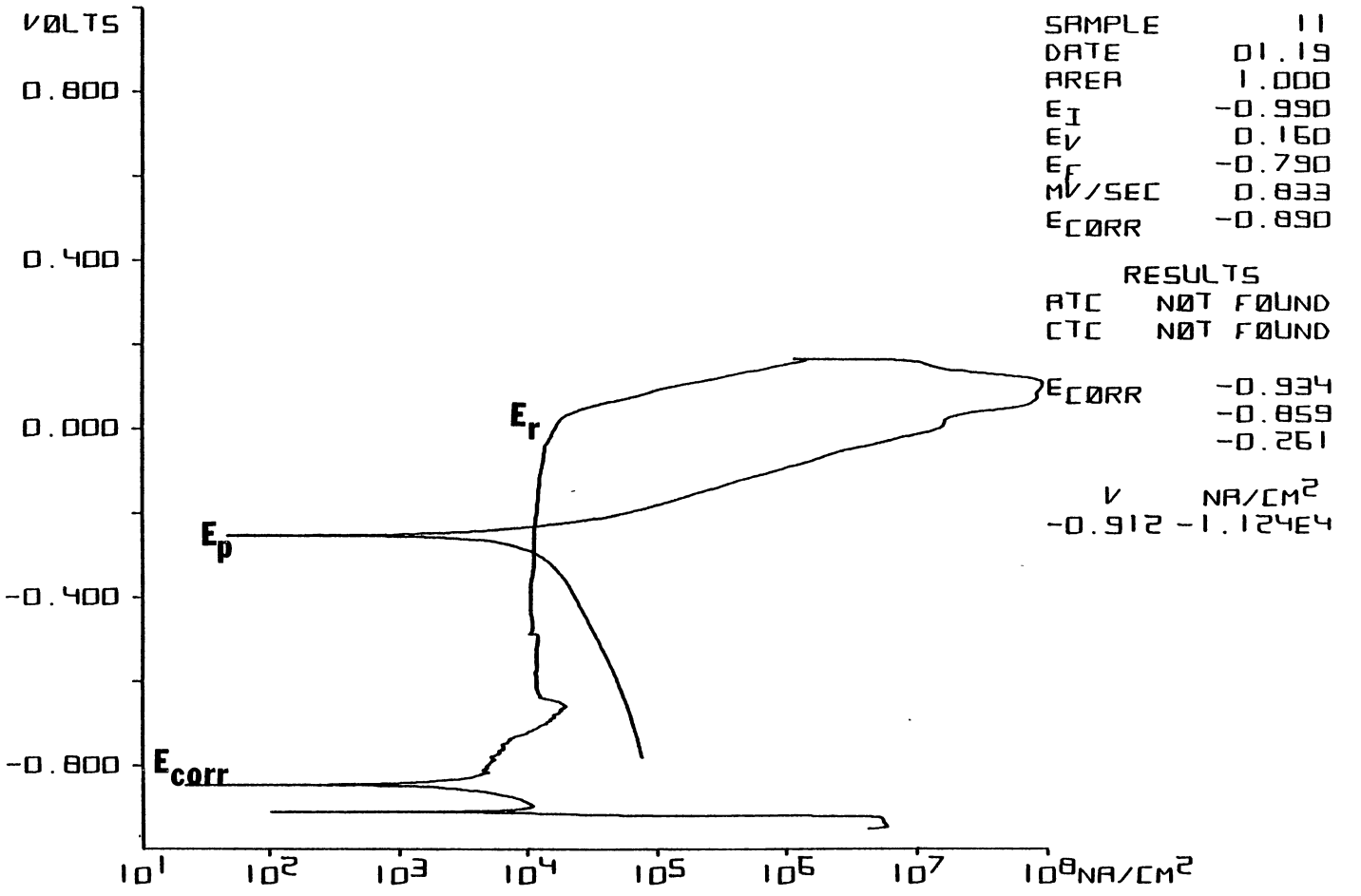

Figure 29 Potentiodynamic Polarization Curve for 304 Alloy, pH = 11.00, 0.1M NaCL, Temperature = 80°C

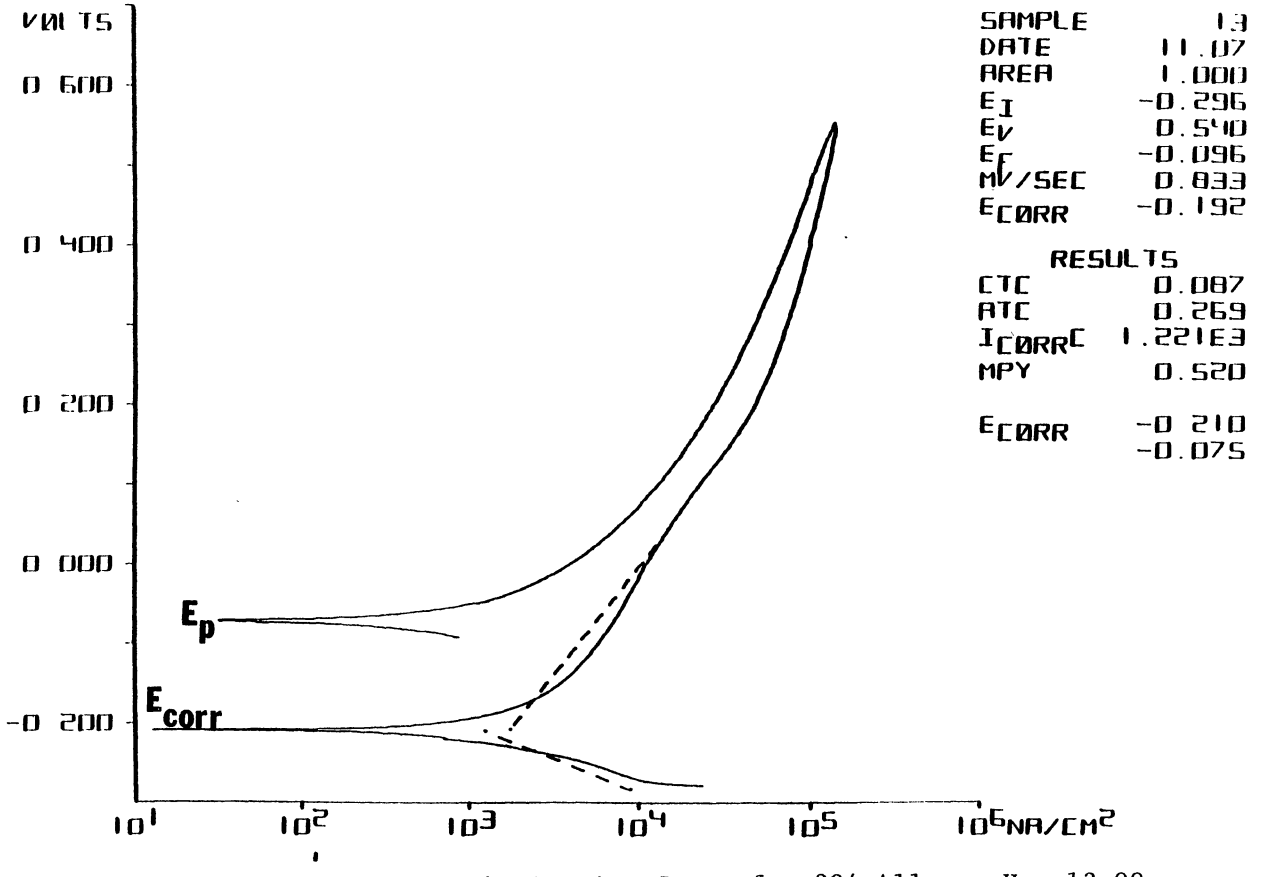

Figure 30 Potentiodynamic Polarization Curve for 304 Alloy, pH = 13.00, Nil-CL^-, Temperature = 80^oC

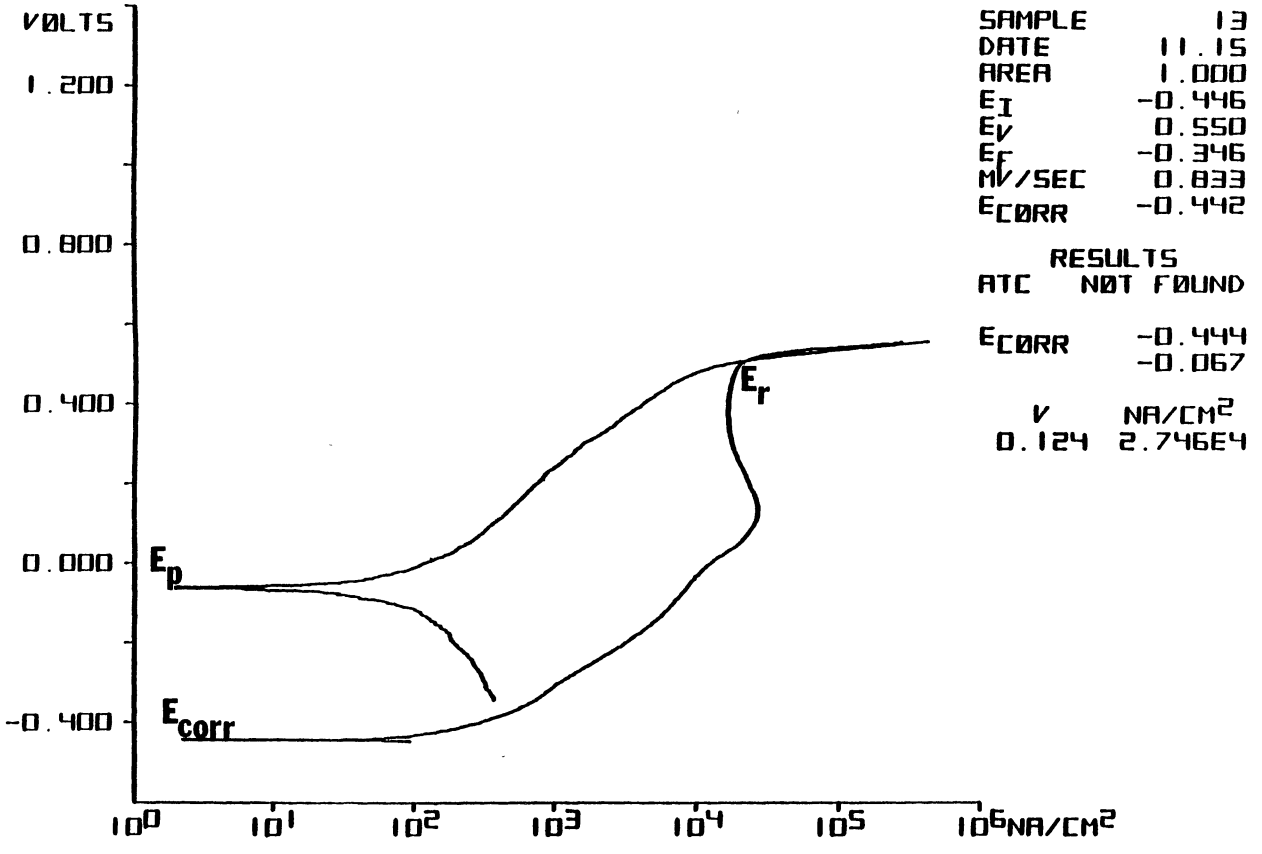

Figure 31 Potentiodynamic Polarization Curve for 304 Alloy, pH = 13.00, 0.1M NaCL Temperature = 80°C

APPENDIX B

CALCULATIONS

APPENDIX B

Calculations of slope of the slanted dashed lines on the Potential-pH diagrams (Figure 20 and 21):

1. Standard cell potential values required to liberate H_2 or O_2 from solutions.

		E^o, Volts
a) to reduce $\overset{+1}{H}$ to $\overset{0}{H_2}$		
pH = 0	$2H^+ + 2\bar{e} \longrightarrow H_2$	0.000
pH = 7	$2H_2O + 2\bar{e} \longrightarrow 2O\bar{H} + H_2$	-0.414
b) to oxidize $\bar{O}^2$ to $\overset{0}{O_2}$		E^o, Volts
pH = 0	$2H_2O \longrightarrow O_2 + 4H^+ + 4\bar{e}$	1.229
pH = 7	$2H_2O \longrightarrow O_2 + 4H^+ + 4\bar{e}$	0.815

2. Using the Nerst equation to calculate E.

Nerst Equation:

$$E = E^o + \frac{RT}{ZF} \text{ In } a_{H^+}$$

$$= E^o + \frac{2.3RT}{nF} \log [H^+]$$

$$E = E^o - \frac{2.3RT}{nF} (pH)$$

where $pH = -\log [H^+]$

$R = 1.98$ cal/gm-mole degree

$T = 353^oK$

$F = 23{,}062 \frac{\text{cal}}{\text{gm-equiv Volt}}$

$$E = E^{o} - \frac{2.3(1.98)(353)\ pH}{n(23,062)}$$

$$E = E^{o} - \frac{0.0697}{n}\ pH$$

a) H_2 evolution line:

pH	E^{o}	n	E
0	0.00	2	0.00
7	-0.414	2	-0.658

$$\text{Slope} = \frac{\Delta E}{\Delta H} = \frac{-0.6580}{7} = -0.0940$$

b) O_2 evolution line:

pH	E^{o}	n	E
0	1.299	2	1.229
7	0.815	2	0.571

$$\text{Slope} = \frac{\Delta E}{\Delta H} = \frac{-0.6580}{7} = -0.0940$$

VITA

Jane-Frances Nannyomo Bakama

Candidate for the Degree of

Master of Science

Thesis: LONG-TERM POTENTIOSTATIC EXPOSURES OF 304 STAINLESS STEEL AT ELEVATED TEMPERATURES

Major Field: Chemical Engineering

Biographical:

Personal Data: Born in Lubanga, Uganda, February 12, 1959, the daughter of Gertulide Nannyonga and Mathias Bakama. Single.

Education: Graduated from Nsube Primary Boarding School, Uganda, in December, 1972; received the East African Certificate of Education (EACE) from Loreto convent in Limuru, Kenya, in December, 1976; received the East African Advanced Certificate of Education (EAACE) from Limuru Girls School, Kenya, in December, 1978. Received Bachelor of Science Degree in Chemical Engineering from Oklahoma State University in May, 1983; completed requirements for Master of Science degree at Oklahoma State University in July, 1985.

Professional Experience: Teaching Assistant, School of Chemical Engineering, Oklahoma State University, August 1983 to May 1985.

Member of: Society of Women Engineers, American Institute of Chemical Engineers, National Association of Corrosion Engineers, and Oklahoma Society of Professional Engineers.